CHALMERS
UNIVERSITY OF TECHNOLOGY

Technical solutions for steam generating heat pumps in industrial applications

A study on steam generation system design based on very high temperature industrial heat pump technology

Master's thesis in Innovative and Sustainable Energy Engineering

LINNEA KARSTEN

DEPARTMENT OF ENVIRONMENTAL AND ENERGY SCIENCES

CHALMERS UNIVERSITY OF TECHNOLOGY
Gothenburg, Sweden 2026
www.chalmers.se

Technical solutions for steam generating heat pumps in industrial applications
A study on steam generation system design based on very high temperature industrial heat pump technology
LINNEA KARSTEN

Department of Environmental and Energy Sciences
Chalmers University of Technology
SE-412 96 Göteborg
Sweden

Acknowledgements, dedications, and similar personal statements in this thesis, reflect the author's own views.

This thesis is done in collaboration with Adven Oy.

SUMMARY

As fossil industrial steam production is being phased out to meet global warming and emission reduction targets, the increasing steam demand needs to be covered by other production methods. As a part of the electrification, steam generating heat pumps can be introduced to industries for efficient steam production based on heat recovery. However, with steam generating heat pumps still entering the commercial market, the availability of literature reviewing installed configurations and solutions is limited. Aiming to fill this gap, this thesis reviews a set of configurations based on closed and open cycle heat pumps as well as the balance of these over a steam separator.

The review of solutions and the optimal balance is conducted by varying the steam generation and separation pressure on which the solutions are designed. This is done for two separate capacity levels and reference processes. The solutions are then evaluated based on total efficiency, or COP, as well as an indicative financial feasibility assessment.

The results suggest that COP is increased with lower steam generation pressures which equates to a solution with closed cycle heat pumps evaporating liquid water at or near atmospheric pressure and subsequently upgrading the steam to the desired conditions using steam compressors, or MVRs. This is mostly in line with commercially available technology, although relatively recently introduced. Furthermore, financial feasibility is dependent on high fuel prices for LFO and natural gas as well as low electricity prices. Emission prices may further improve the business case. These findings suggest that steam generating heat pump may be a realistic alternative for industrial steam generation for low pressure requirements in the Nordic region where price profiles are financially beneficial.

Keywords:

Steam Generating Heat Pumps, Electrification, VHTHP, MVR, Industry

Table of contents

Preface and acknowledgements

Writing a master's thesis is something that had felt like an enormous undertaking and a bit of an impossible task for me prior to starting the work, but with the support and help of my colleagues, friends, and most of all my family, I am happy and proud to have completed it. It would genuinely not have been possible without you!

In writing my thesis I am happy to have learnt a lot about both heat pump technologies and industrial steam generation, but more importantly the work has taught me how to work on and manage a project and given me insights and new perspectives on industrial energy production, both from an academic and business point of view.

Studying and doing my master's in a Nordic double degree program has been an incredible journey full of new friends and opportunities, although not without its ups and downs. Nevertheless, the project of writing my master's thesis for two schools in separate countries has been nothing but rewarding and I want to thank my examiner prof. Simon Harvey at Chalmers University of Technology and supervisor Henrik Holmberg at Aalto University for all the support, collaboration, and making this project a really positive experience.

I am also fortunate to have had the opportunity to write my thesis for Adven Oy on a topic so interesting and relevant in today's world and to do that with amazing colleagues who have supported and cheered me on throughout this project. Thank you to everyone at Adven and especially to my advisor Timo Puputti and manager Pasi Kolehmainen for the guidance and encouragement all the way from planning to submission.

Thank you!
Tack!
Kiitos!

Symbols and abbreviations

Symbols

T	Temperature
p	Pressure
h	Enthalpy
s	Entropy
V	Volume
η_{is}	Isentropic efficiency
η	Overall efficiency (excluding η_{is})
$\dot{m}$	Mass flow
v	Specific volume
P	Power
W	Work
Q	Fuel/Energy amount
c	Energy cost

Abbreviations

CFC	Chlorofluorocarbons
COP	Coefficient of Performance
GWP	Global Warming Potential
HC	Hydrocarbons
HFC	Hydrofluorocarbons
HTHP	High Temperature Heat Pump
IEA	International Energy Association
KPI	Key Performance Indicator
LFO	Light Fuel Oil
MVC	Mechanical Vapor Compression
MVR	Mechanical Vapor Recompression
NG	Natural Gas
NZE	Net zero Emissions by 2050 Scenario by the IEA
ODP	Ozone Depletion Potential
SGHP	Steam Generating Heat Pump
SSC	Single Screw Compressor
TRL	Technology Readiness Level
TSC	Twin Screw Compressor
TVR	Thermal Vapor Recompression
VHTHP	Very High Temperature Heat Pump

Use of Artificial Intelligence

Artificial intelligence in the form of Copilot has mainly been used in this thesis for creating and correcting MATLAB code for the purpose of illustrating the SGHP solutions in log p-h diagrams. Furthermore, it has been used to some extent as an aid in understanding technology or different principles. Experience-based assumptions made in the context of, for example, compressor efficiencies have been verified to be realistic using AI.

Since no information or data has been taken directly from AI and a sensitivity analysis was conducted on the least certain coefficients, the use of artificial intelligence is assessed to not have affected the outcomes and results of the thesis. The diagrams illustrated based on the code created by Copilot were also verified to portray the accurate processes and points. Additionally, no artificial intelligence has been used to produce text or correct text in this thesis beyond what may be integrated into the language check in Microsoft Word.

1 Introduction

Industrial processes within many different sectors are major consumers of energy. The main form of energy used in industry is steam as it is a good energy carrier, easy to source, and non-toxic. Historically, the steam consumed in industry has been produced through combustion of, for example, coal or oil, with its roots in the industrialization. As environmental and energy related regulations tighten in hopes of combatting climate change, fossil fuels are being phased out, and new technologies and energy sources are introduced to the market to cover the growing demands on the energy market. One technology that is believed to grow to fill a part of this vacancy is heat pumps capable of steam production, or steam generating heat pumps. Steam generating heat pumps are developed in many parts of the world with both pilot and commercial installations already in operation today.

This thesis aims to examine the state-of-the-art of steam generating heat pumps as well as the integration of steam generating heat pumps into industrial processes. Possible integrations are evaluated through concept level designs for steam generation systems and key performance indicators (KPI) for the processes including COPs. As a result, the main research question of this thesis is how steam generating heat pumps can be integrated into industrial processes in the most technically and financially feasible and sound way as well as finding possible limitations to the applications.

This thesis does, however, not consider all possible steam generation system concepts and does therefore not draw exclusive conclusions on the relation and comparison between the reviewed system designs and other solutions that may also be alternatives for the processes. While the literature review covers a wide range of solutions and equipment for heat pump-based steam generation, the evaluated designs and configurations have a clear focus on closed cycle heat pumps, steam separators and MVRs. This focus is motivated by an identified scarcity of similar studies made. Detailed economic evaluation of the reviewed systems is, however, not included in the scope of evaluation of the solutions. Furthermore, as the designs are on a concept level, detailed installation design, including but not limited to piping, is not considered.

To conclude, this thesis aims to provide an indication on steam generation system designs in industrial processes of two different power levels as current literature on design choices in steam generating heat pumps is limited. The work is divided into two main sections. A literature review, presented in chapter 2, and an evaluation of SGHP designs. The methodology for the latter section is presented in chapter 3 along with the reference processes considered. Chapter 4 presents the results of the study both from a technical and basic financial perspective along with a discussion of them. Final conclusions are then drawn in chapter 5.

2 Literature review

The purpose of the literature review is to examine the current development of steam generating heat pumps and the state-of-the-art, while also reviewing technologies and solutions currently available on the market. The material used for this includes both scientific articles and product documentation from suppliers, however, it is not limited to these categories. The following paragraphs outline the methods for the literature review closer.

The general overview of steam generating heat pumps and state-of-the-art are mainly based on published scientific articles. Due to the concept of steam generating heat pumps, mainly VHTHP and MVR, as well as electrification of industrial processes being relatively new compared to the history of the industries and steam cycles themselves, special attention is paid to the date and year of publication for the articles. Since development of these technologies is rapid the aim is to primarily review articles published in the last 5 years, however, with some exceptions. In addition to scientific articles, some historical data and information on the energy market development by the IEA is utilized to depict a reference scenario for the electrification.

Suppliers and products that are active on the market are also mentioned to some extent in scientific articles, however, the main source of information for specific product technologies and companies is the websites of these companies or technical data sheets etc. Additionally, some marketing material and product brochures are used when available.

Following chapters elaborate on the industrial energy status as well as steam generation in the industry with a focus on steam generating heat pumps and the different technologies and configurations available in chapters 2.1 and 2.2, respectively, a more specific look at mechanical vapor recompression (MVR) in chapter 2.3 and finally available evaporation technologies in chapter 2.4.

2.1 Industrial energy consumption today

The industrial sector is a major actor and consumer on the global energy market, covering a significant share of the energy consumed every year. According to the International Energy Agency (IEA) the energy consumption of the industrial sector reached 166 EJ ($166 \cdot 10^{12}$ MJ) in 2022, which is equivalent to 37% of all energy consumed globally that year (IEA, 2023a). Additionally, out of the 166 EJ consumed approximately two thirds were fossil fuels including coal, oil, and gas (IEA, 2023a). These numbers highlight the weight and importance of the industrial sector in the fight against climate change and mitigation actions needed to meet targets of climate neutrality by 2050. To illustrate the pathway to climate neutrality and reflect the

development needed to meet these targets, the IEA have created a 'Net Zero Emissions by 2050 Scenario' (NZE) as well as corresponding targets for 2030. To follow up the real development in relation to the NZE the IEA also developed a 'Tracking Clean Energy Progress'-report with the lates updates available from 2023 (IEA, 2023b). The progress report assigns all eight sectors along with their respective subsectors a classification out of the three classes, 'On track', 'More effort needed', and 'Not on track', based on the current state of development in relation to the 2030 targets. As one of the eight sectors, the industry is tracked on six different subsectors, including steel, chemicals, cement, aluminum, paper, and light industry, with five out of the six subsectors assigned 'Not on track'.

An important part of decarbonizing industrial processes is replacing fossil fuels with zero or low emission electricity, also referred to as electrification. Since the main use of fossil fuels in the industry is steam generation through combustion in industrial boilers, the electrification to cover this demand can either be direct, such as electrical boilers or heat pumps for example, or indirect electrification through electrolysis and hydrogen production or production of other synthetic fuels(Wei et al., 2019). The synthetic fuels can then be combusted to generate steam similarly to the fossil fuels, however, excluding fossil CO_2 emissions as well as other air pollutants that fossil fuel combustion would generate.

Electrifying industrial processes has, however, proven difficult and less competitive than required for climate neutrality targets to be met. An article published in 2019 claimed that the industrial sector would be "one of the most difficult sectors to decarbonize"(Wei et al., 2019), referring to electrification related challenges such as connection to the electric grid, the competitiveness with significant capital investments for the process modification and high temperature and pressure requirements for the steam in many processes. Since the year 2019 significant development has taken place regarding electricity prices, for example in Europe, with volatility increasing due to a larger share coming from renewable energy production while international and political circumstances restrict fuel availability.

2.2 Steam generating heat pumps

Heat pumps have been popular in heating applications with lower target temperatures for some time; however, recent development have increased their relevance also within the industry with state-of-the-art target temperatures now suitable for steam production purposes as well. Simultaneously, heat pumps offer a means of reusing excess heat from the processes that had otherwise been lost. This also means the specific electricity consumption per unit of delivered heat decreases compared to an electric boiler. When talking about heat pumps able to deliver sufficient temperatures for

steam production, they are often referred to as High Temperature Heat Pumps (HTHP) or Very High Temperature Heat Pump (VHTHP), while heat pump for the specific purpose of steam production are referred to as Steam Generating Heat Pumps (SGHP) (Klute et al., 2024). Klute et al. define the High Temperature Heat Pumps as delivering temperatures above $80°C$ while Very High Temperature Heat Pumps can deliver temperatures above $100°C$.

Heat pumps can further be divided into Closed Cycle Heat Pumps and Open Cycle Heat Pumps reflecting the configuration of the refrigerant cycle in the heat pump (Klute et al., 2024). Furthermore, closed and open loop heat pumps can be divided into subclasses depending on the technology and the principles the technology is based on according to Figure 1; however, this will be reviewed in more detail in the following sections 2.2.1 and 2.2.2. Finally, closed and open cycles can be combined in series to achieve the desired steam conditions. The different configurations are further presented in section 2.2.3.

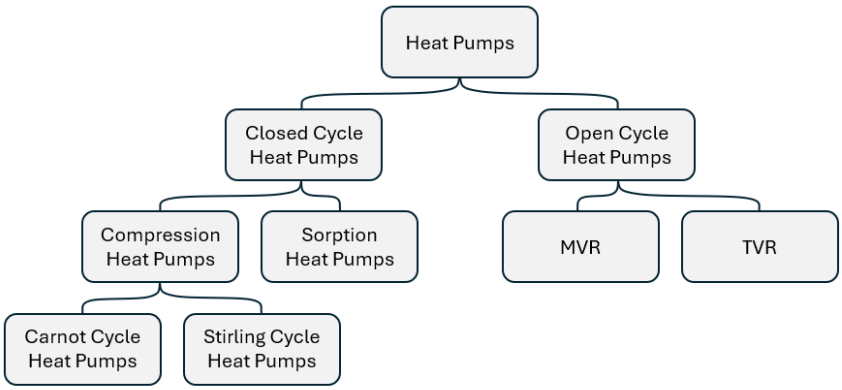

Figure 1: Heat pump technology classes.

2.2.1 Closed cycle heat pumps

Closed cycle heat pumps refer to a specific type of heat pump that uses a separate cycle with working fluid, or refrigerant, between the heat source and heat sink. The refrigerant cycle is connected to the heat source and -sink through two heat exchangers or one evaporator and one condenser depending on the working fluid. One major subcategory of closed cycle heat pumps are compression heat pumps, which can operate on, for example, a Stirling- or Carnot-cycle and subsequently offer different properties and possibilities for the heat pumps (Klute et al., 2024). Figure 2 illustrates the theoretical and basic Carnot- and Stirling-cycle in a ph-diagram and pV-diagram, respectively.

Figure 2a) represents the Carnot-cycle where the refrigerant alternates between two phases as it evaporates and condenses in the heat exchangers at the heat source and heat sink. The cycle consists of four basic thermodynamical processes (Suong and Asanakham, 2020). Between points 1-2 the refrigerant saturated vapor is compressed, which increases both the temperature and pressure, as well as the enthalpy, of the vapor. From point 2-3 the superheated refrigerant vapor is condensed to saturated liquid at the heat sink heat exchanger. The saturated liquid is then expanded from point 3-4 which decreases the pressure and temperature of the refrigerant. However, some evaporation is taking place at this stage already as can be seen from point 4 being located within the saturation dome. Finally, the low-pressure refrigerant is evaporated to saturated vapor between points 4-1, which takes place in the heat source heat exchanger.

Similarly, Figure 2b) depicts the process cycle of Stirling heat pump, although, noting that the horizontal axis of the graph is referring to the volume instead of enthalpy. The main difference between a Carnot-cycle compression heat pump and a Stirling-cycle one is the lack of phase changes for the refrigerant in a Stirling heat pump. Instead the gaseous refrigerant undergoes four thermodynamical processes in a theoretical cycle (Minale et al., 2024). Between points 1-2 the gas is compressed into a smaller volume and subsequently the pressure of the gas increases. The compressed refrigerant is then cooled down from point 2-3 in a constant volume which also lowers the pressure. Between points 3-4 the cooled down gas is expanded into the larger initial volume which results in additional pressure decrease from point 3. Finally, the refrigerant is heated up from point 4-1 which again increases the pressure. The heating and cooling between points 4-1 and 2-3 takes place in a regenerator located between the two cylinders of the Stirling heat pumps where heat is stored as the refrigerant passes from one cylinder to the other (Minale et al., 2024). The heat pump is then connected to a heat source and a heat sink through heat exchangers between points 3-4 and 1-2, respectively (Minale et al., 2024). This keeps the refrigerant temperature constant as the excess heat produced in the compression is transferred to the heat sink and vice versa for the expansion.

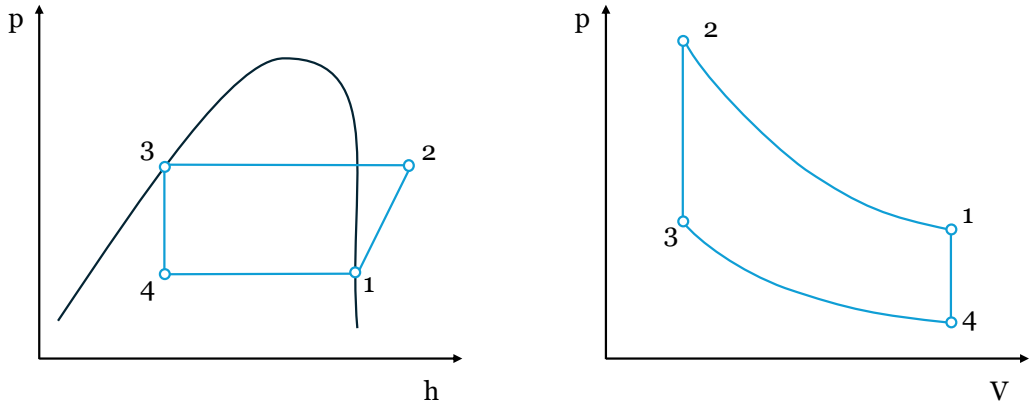

a) b)

Figure 2: Theoretical and basic illustrations of a) a Carnot heat pump cycle in a ph-diagram (Suong and Asanakham, 2020) and b) a Stirling heat pump cycle in a pV-diagram (Minale et al., 2024)

A crucial part of a closed cycle compression heat pump is the refrigerant it uses. The refrigerant selection for a heat pump is made both based on the desired temperature targets and high efficiencies as well as environmental and safety aspects (Arpagaus et al., 2018). The boiling point of a fluid at different reasonable pressures is one physical property to consider ensuring that a Carnot-cycle heat pump can reach the required temperatures. Exact temperatures can be met by adjusting the pressure levels on the condenser and evaporator, however, there are some restrictions to this possibility. The evaporator pressure is not to be lower than the ambient air pressure to exclude the risk of surrounding gases or air leaking into the refrigerant system, while the condenser pressure should not be too close to the critical point pressure level of the fluid, which would result in smaller enthalpy differences at condensation (Arpagaus et al., 2018).

Some synthetic refrigerants have significant negative environmental impact, which are usually divided into ozone depletion potential (ODP) and global warming potential (GWP). Due to this synthetic and environmentally harmful refrigerants, such as chlorofluorocarbons (CFCs) or hydrofluorocarbons (HFCs), are being phased out, or already banned from the market, under both global and European protocols and regulations (Arpagaus et al., 2018). Instead, natural refrigerants, including hydrocarbons (HCs), water, and gases such as hydrogen, helium, air or nitrogen, are gaining popularity. Several of the natural refrigerants do, however, have high flammability, including some hydrocarbons and hydrogen, requiring additional safety measures for heat pumps with these working fluids (Arpagaus et al., 2018).

Both Carnot- and Stirling-cycle heat pumps can be used for steam generation, however, supply temperatures, capacities and technology readiness levels (TRL) of currently available solutions vary (Klute et al., 2024). The TRL of a solution refers to the state at which the development of the technology or product is, ranging from basic concepts or principles at TRL1 to working and proven systems at TRL9 (Manning, 2023). Although the development of steam generating heat pumps is still in quite early stages, there are suppliers achieving high TRLs on the market today.

Table 1: Suppliers of closed cycle compression heat pumps.

Producer	Current capacity	Supply temperature	Corresponding steam pressure	Source
Heaten	2.5 MW	180 $°C$	10 $bara$	(Heaten, n.d.–a)
Enerin AS	0.5 MW	250 $°C$	40 $bara$	(Enerin AS, n.d.–a)

One example of a VHTHP using a Carnot-cycle compression heat pump is the HeatBooster by Heaten. The German company advertises steam supplies at the capacity and pressure level presented in Table 1 with the current model using hydrocarbons as the refrigerants and heat sources of $10 - 150°C$, while soon to be launched models would have a capacity of up to 10 MW_{th} with the same steam conditions and refrigerants (Heaten, n.d.–a). Since these HeatBooster models use natural refrigerants, they are not subject to phase out under the restrictions presented above. The concept of the HeatBooster steam generating heat pump is steam generation directly at the heat sink heat exchanger, meaning that the feed water evaporates as the refrigerant condenses (Klute et al., 2024). An image of the heat pump is presented in Figure 3a). Heaten has also reached high TRLs of 7-9 already with the technology itself having achieved a TRL9 (HPT TCP, 2023).

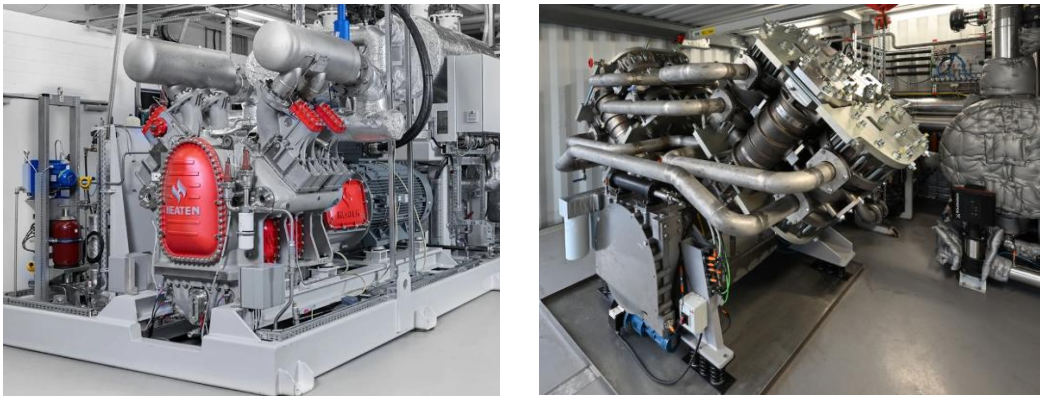

a) b)

Figure 3: Installed closed cycle compression heat pumps by a) Heaten (Heaten, n.d.–b) and b) Enerin AS (Enerin AS, n.d.–b).

When it comes to steam generating Stirling-cycle heat pumps, one example of a supplier is Enerin AS with the HoegTemp VHTHP. With their V6 model, Enerin advertises supply conditions according to Table 1, while a V12 model is also available doubling the capacity (Enerin AS, n.d.–a). The supply temperature, however, refers to the pressurized hot water produced by the heat pump as the steam production occurs in a separate steam generator connected to the HoegTemp heat pump by a closed water circuit (Klute et al., 2024). Since the heat pump uses a Stirling-cycle the working fluid is gaseous and in the case of HoegTemp, helium works as the refrigerant (HPT TCP, 2022a). Helium is also included in the natural refrigerants meaning that, similarly to the HeatBooster, Enerin's HoegTemp heat pump is not subject to phase out. Furthermore, helium is inert and not flammable, so additional fire safety measures are not required. Enerin and the HoegTemp heat pump has achieved TRL6 (HPT TCP, 2022a). However, several pilot sites from previous years are presented among their references, including steam generating systems (Enerin AS, n.d.–b). An installed HoegTemp heat pump can be seen in Figure 3b) with the separate steam generator visible on the far-right side of the image.

In addition to compression heat pumps, the area of closed cycle heat pumps also covers sorption heat pumps. Sorption heat pumps utilize an external heat source in addition to the waste heat and electricity, typically resulting in a total $COP < 1$ (Klute et al., 2024). Additionally, their influence on the European market has been insufficient for continued and determined development in Europe (Klute et al., 2024). They are, however, not directly comparable to compression heat pumps in terms of COP due to technological differences and with their lower popularity on the European market, sorption heat pumps are not reviewed further in this thesis.

2.2.2 Open cycle heat pumps

Open cycle heat pumps differ from previously reviewed closed cycle heat pumps in that, as the name suggests, the system does not contain a separate and isolated loop of a working fluid between the heat source and the heat sink. Instead, the working fluid or process medium, which in the case of steam generating heat pumps would be steam, is directly upgraded in the heat pump (Klute et al., 2024). The fact that open cycle heat pumps do not use refrigerants also means that refrigerant regulations and limitations do not affect or limit the development and installation of these heat pumps. Generally, open cycle heat pumps cover two main technologies, mechanical vapor recompression (MVR) and thermal vapor recompression (TVR) (Klute et al., 2024).

Mechanical vapor recompression (MVR) refers to upgrading and pressurizing steam through mechanical means including compressors and blowers (Ma et al., 2024). MVR technologies are based on the principle of increasing the pressure of steam either though pushing the medium into a smaller volume or increasing the speed of the flow. The theoretical thermodynamical process of MVRs can be seen in Figure 4. The process is presented in a Ts-diagram with dashed purple lines illustrating the isobaric lines. The compression process itself is presented in blue as the steam is compressed from point 1 to point 2 with the straight vertical line indicating that the theoretical compression is isentropic, meaning no change in entropy and thus also adiabatic. This process is similar to the compression of the refrigerant prior to the condenser in a closed cycle heat pump. Additionally, the graph illustrates that

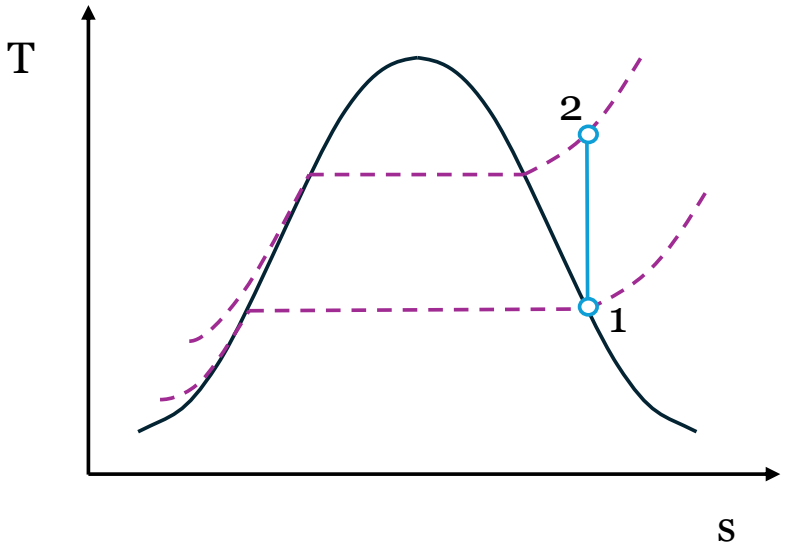

Figure 4: Theoretical compression of steam presented in a Ts-diagram (Suong and Asanakham, 2020)

MVRs increase both the pressure and the temperature of the steam which upgrades the steam to higher enthalpies and thus suitable for use in applications requiring higher grade steam. It is also worth noting that the compression occurs completely on the right-hand side of the saturation dome implying that no water droplets are present. Specific MVR technologies as well as suppliers and TRLs will be further reviewed in chapter 2.3.

The second type of open cycle heat pumps, thermal vapor recompression (TVR), operate using thermal power to increase the pressure of a steam flow. A TVR is connected to two steam flows, one high pressure steam flow and one low pressure steam flow which is to be upgraded (Klute et al., 2024). As the high-pressure steam enters the TVR with high velocity it creates a suction which pulls in the lower pressure steam thus increasing the speed and pressure of this secondary flow. Since the driving force of the TVR is thermal and not mechanical, it also means that a TVR does not consume electricity and is therefore not directly related to electrifying industrial processes. Additionally, the TVR requires high pressure, and thus high temperature steam to function, which would likely come from more traditional fuel boilers. Due to these reasons, TVRs are not further considered or reviewed in this thesis.

2.2.3 Combinations of heat pump technologies

Steam generating heat pumps are often a combination of technologies and closed- and open-cycle heat pumps coupled in different configurations to build a system that can achieve the desired steam conditions in the best possible way. Klute et al. identified five general concept classes to cover general configurations of different heat pump technologies (Klute et al., 2024). The identified concept classes were labeled SGHP-A to SGHP-E and are compiled in a graphical representation visible in Figure 5. The technology group ‘Closed HP’ refers to closed-cycle heat pumps covering both compression and sorption heat pumps. Similarly, ‘Open HP’ refers to open-cycle heat pumps including both MVRs and TVRs. The group ‘Evaporator/Flash’ covers separate steam generator technologies including evaporators and flash tanks or vessels. Evaporators refer to steam generators where water is evaporated by adding heat to it, while flash vessels evaporate the water by suddenly decreasing the pressure, thus lowering the boiling point of the water enough for it to evaporate at its current temperature. Evaporation technologies will be further reviewed in chapter 2.4. The concept classes SGHP-A to SGHP-E are described in following paragraphs along with flow diagrams illustrating the concept configurations. In the flow diagrams, red lines are used to portray gas/vapor phase fluid flows while blue lines portray mainly liquid fluid flows.

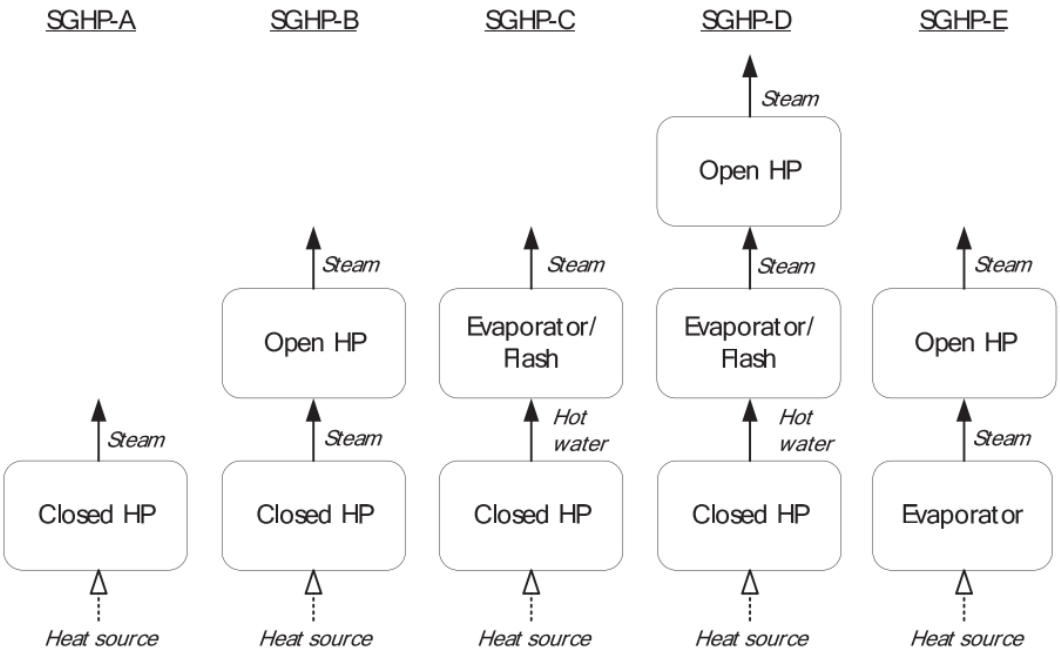

Figure 5: General SGHP configurations and concept classes as presented by Klute et al. (Klute et al., 2024)

The concept class SGHP-A includes systems with only a closed-cycle heat pump and where the steam generation occurs already in the heat sink heat exchanger of the heat pump. A flow diagram of this concept is presented in Figure 6. One example of a heat pump included in this class is the Heaten HeatBooster presented earlier (Heaten, n.d.–a). Out of 20 heat pumps or solutions reviewed by Klute et al. for this concept class, 15 were compression heat pumps while the remaining five were sorption heat pumps (Klute et al., 2024). These solutions had achieved TRLs spread over the whole scale of 1-9 and thermal capacities varied greatly.

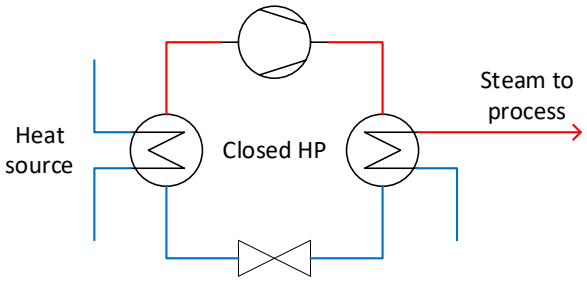

Figure 6: Flow diagram of a SGHP-A concept configuration.

The concept class SGHP-B covers solutions where closed cycle heat pumps from the first class, SGHP-A, are combined with open-cycle heat pumps to further upgrade the steam to higher pressures. This configuration is illustrated in a flow diagram in Figure 7. For this class Klute et al. reviewed nine solutions (Klute et al., 2024). Out of these nine, seven solutions were combinations of closed cycle compression heat pumps and MVRs. The other two used TVRs for the steam compression, one in combination with a compression heat pump and the second with a sorption heat pump. The solutions in this concept class also had TRLs over much of the scale, however, the solutions including MVRs generally had lower TRLs compared to the TVR.

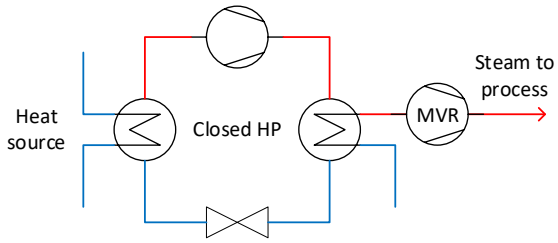

Figure 7: Flow diagram of a SGHP-B concept configuration with an MVR-type open heat pump.

Contrary to the first two concept classes, SGHP-C covers solutions where the closed cycle heat pump does not produce the steam directly but supplies hot water to either a flash vessel or evaporator, as demonstrated in Figure 8. All solutions reviewed by Klute et al. in this class use compression heat pumps, however, there are two distinct types of solutions with Carnot-cycle heat pumps in combination with flash vessels and Stirling-cycle heat pumps in combination with evaporators (Klute et al., 2024). Of these two types, they have reviewed five and two solutions, respectively, which have relatively high TRLs with all seven being > 5. The HoegTemp heat pump by Enerin is one example of steam generating heat pump solutions in this concept class.

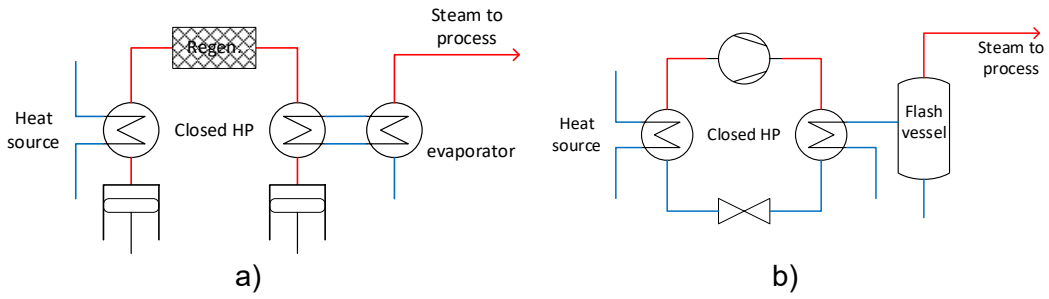

Figure 8: Flow diagram of SGHP-C concept configuration with steam generation in a) an evaporator connected to a Stirling heat pump and b) a flash vessel connected to a Carnot heat pump.

The fourth concept class SGHP-D combines the previous classes by covering solutions with closed-cycle heat pumps producing hot water which is then directed to a flash vessel or evaporator and finally the steam is upgraded with open-cycle heat pumps. All three solutions reviewed by Klute et al. in this class were configurations of compression heat pumps, flash vessels and MVRs with largely varying TRLs (Klute et al., 2024). Figure 9 shows the configuration of these heat pumps in a flow diagram.

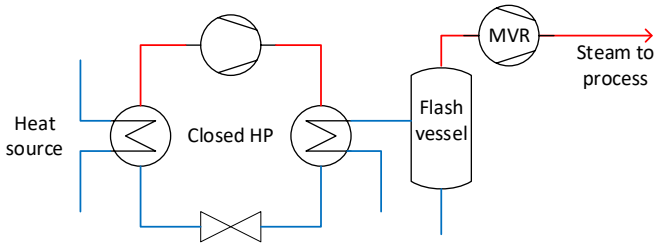

Figure 9: Flow diagram of SGHP-D concept configuration with a flash vessel and MVR.

Finally, the last concept class SGHP-E differs from the previous four classes in that these solutions do not include a closed-cycle heat pump. Instead, steam is directly produced in an evaporator without being heated first and then upgraded using an open-cycle heat pump as illustrated in Figure 10. All four solutions reviewed by Klute et al. were evaporator-MVR configurations of which two had achieved a TRL9 while the remaining two were at the lower end of the scale (Klute et al., 2024).

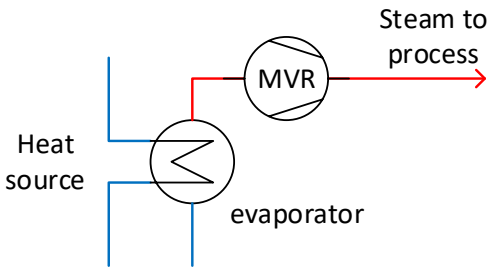

Figure 10: Flow diagram of SGHP-E concept configuration.

Although this classification covers most of the generally used configurations of steam generating heat pumps, some solutions remain outside of the concept classes. One example is a system where pressurized hot water coming directly from the process is flashed in a flash vessel followed by an open-cycle heat pump, for example an MVR, to increase the pressure back to the desired steam conditions. This is close to what the last class SGHP-E covers, however, since it only refers to evaporators this scenario is excluded. Another example of a system outside the five classes is low pressure steam from the process directed to an open-cycle heat pump to upgrade the steam back to desired conditions without the need for a bottom cycle or evaporation.

2.3 Mechanical vapor recompression

As the name suggests, mechanical vapor recompression (MVR) refers to increasing the pressure of vapor or steam through mechanical means. MVRs are, as mentioned above, within the area of open cycle heat pumps and often a central part of steam generating heat pump configurations. Today MVRs are used in several applications including desalination and waste water treatment processes (Han et al., 2021). In these cases, the configuration looks somewhat different from installation in a steam generating heat pump, however, the steam compressor itself is assumed to function the same in both applications. Additionally, the literal interpretation of MVRs indicates that only applications where the compressor is recompressing already consumed low pressure steam to bring it back up to useful temperatures are included in the terminology. Thus, applications where previously produced steam is upgraded using a steam compressor would be referred to as mechanical vapor compression or MVC. Some literature uses this distinction, however, as the term MVR is widely understood to cover both types of applications, the abbreviation is also used for all steam compression applications in this thesis.

MVRs usually utilize one of two principles to increase the pressure of the steam stream. The steam can either be compressed into a smaller volume, thus increasing the pressure, or increase the speed of the stream, which has a similar increasing effect on the pressure of the steam (Ma et al., 2024). Volume-type compressors include several technologies, such as piston compressors where steam is compressed in cylinders, as well as rotary compressors that utilize rotating components to compress the steam (Ma et al., 2024). Some examples on rotary compressors are scroll, root, screw, and twin-screw compressors. Speed-type compressors, that are in some cases also referred to as MVR blowers or fans, can also be further categorized into axial flow or centrifugal blowers and are usually the preferred terminlogy for lower pressure increases while compressors can create larger lifts in pressure (D'Alessandro et al., 2025). When reviewing MVR technologies Klute et al. found

that screw and turbo compressors were the most common in steam compressor applications, with turbo compressors referring to for example centrifugal blowers, although piston compressors are also used for high supply temperatures (Klute et al., 2024). Similarly, Ma et al. found that water vapor compression is mainly concentrated to technologies like centrifugal, roots, and screw compressors (Ma et al., 2024). Based on these assessments, piston, screw, and centrifugal compressor technologies are closer reviewed in following subchapters along with examples on suppliers and manufacturers of these compressor types.

2.3.1 Piston steam compressor

Piston compressors, as volume-type compressors, increase the pressure of the steam by decreasing the available space it can occupy. Piston compressors consist of a number of cylinders with their respective pistons connected to a common crankshaft which is driven by an electric motor (Ma et al., 2024). Furthermore, the cylinders have inlet and outlet ports through which the low pressure steam is let into the cylinder when the piston moves down with the crankshaft, and the compressed steam is let out when the piston is nearing its highest point in the cycle. In this type of piston compressor, one rotation of the crankshaft compresses one cylinder worth of steam in each cylinder. Double-acting piston compressors, however, have inlet and outlet ports both at the top and bottom of the cylinder which means that steam can be compressed on both sides of the piston (Spilling, 2024a). As the piston compresses the steam above it, low pressure steam enters the cylinder below the piston as that space increases and is then compressed as the piston moves back down allowing low pressure steam to enter the upper part of the cylinder again. This set-up lets the piston compressor work on two units of steam simultaneously, resulting in two cylinders worth of steam being compressed for each rotation of the crankshaft. An illustration of a double-acting compressor is presented in Figure 11.

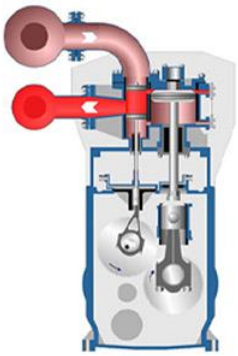

Figure 11: Working principle of piston compressor by Spilling (Spilling, 2024a).

One supplier that manufactures double-acting piston steam compressors is the German company Spilling (Spilling, 2024b). The Spilling steam compressor can include up to 6 cylinders per unit with sizes customized to the steam demands (HPT TCP, 2022c). The inlet and outlet pressure limitations of this compressor are presented in Table 2, with the maximum outlet pressure corresponding to saturated steam at $250\,°C$. One compressor in which pressurization takes place in two stages can reach a maximum total pressure ratio of 6 (Spilling, 2024a). However, larger pressure lifts can be accomplished with multiple compressors in series. The mass flows that can be compressed with the Spilling compressor are in the range of $1 - 20\,t/h$ (Spilling, 2024b). As a result, Spilling's piston compressor can reach high pressure ratios in only a few stages and is suitable for small to medium sized industrial processes.

Piston compressors reviewed by Ma et al., covering 19 technologies, all work on vapors from other refrigerants than water, mainly HFOs and HCs (Ma et al., 2024). This indicates that piston compressors are rarely used specifically for steam compression. The Spilling piston compressor is, however, advertised to specifically be intended for use in steam compression (HPT TCP, 2022c). This compressor has already achieved a TRL9 and is advertised to be in use at several plants. Nevertheless, the development of piston compressors face one main issue to be solved, the seals between the cylinder walls and pistons to ensure no leakage occurs when the vapor is compressed (Ma et al., 2024). This is, however, not solely valid for piston steam compressors but an issue for other technologies as well.

2.3.2 Screw steam compressor

Screw compressors utilize, as the name suggests, one or two rotating screws to compress steam and therefore fall under the rotating volume-type compressor category. The two screw compressor types with one and two screws are single screw compressor (SSC) and twin screw compressor (TSC), respectively (Ma et al., 2024). In steam compression and MVR applications both types are used as is indicated by the multiple technologies reviewed by Ma et al (Ma et al., 2024). Generally, screw compressors are best suited for lower mass flows and thus smaller scale MVR systems (Liu et al., 2019). Following paragraphs will review the configurations of these compressors along with manufacturers and screw compressors on the market.

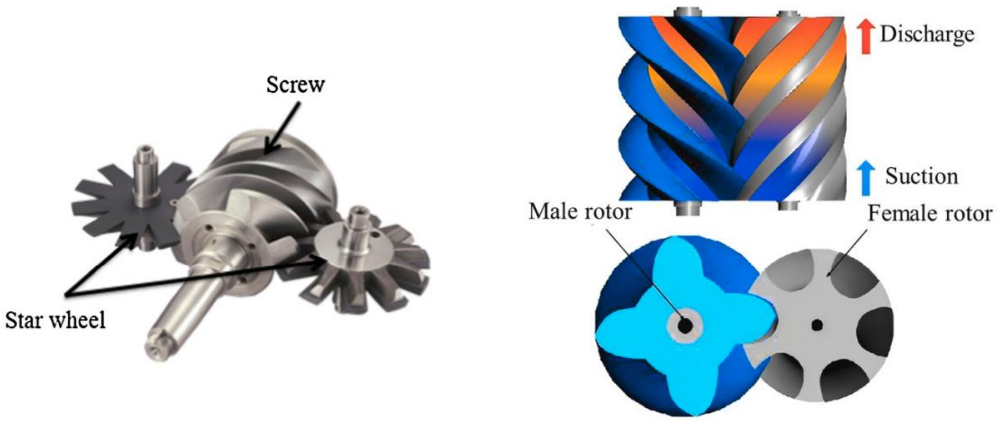

Figure 12: The configurations of a) a single screw compressor (Yang et al., 2016) and b) a twin screw compressor (Ma et al., 2024).

Single screw compressors (SSC) consist of one screw and two star wheels (Yang et al., 2016). Additionally, the screw is incased in a casing and connected to an electric motor which drives the screw to rotate (Ma et al., 2024). The screw's rotations in turn drive the star wheels to rotate. This structure is also visible in Figure 12a). The compression of the steam itself takes place in the grooves of the screw within the casing. As can also be seen in Figure 12a), the depth of the grooves is decreasing towards the back of the screw which also results in the volume between the screw and the casing decreasing, thus compressing the steam within. The star wheels help push forward the steam and compress it as the screw turns.

A twin screw compressor differs most from an SSC in that it has two screws instead of one as well as no star wheels. The two screws are, however, not identical. Instead, it has so called male and female rotors, that fit together as they rotate, in addition to the shell and electric motor (Liu et al., 2019). This is also visible in Figure 12b). Similarly to an SSC, the steam is compressed in the grooves of the female screw and in the spaces between the two screws (Ma et al., 2024).

The performance of both single and twin screw compressors can be significantly improved with de-superheating using water injection in the compression stage (Liu et al., 2019, Yang et al., 2016). A study made with an SSC found that by injecting water while compressing the steam, the enthalpy difference on the compression decreases and the pressurized steam is closer to the saturation dome and not considerably superheated (Yang et al., 2016). Since the enthalpy difference in the steam is lower, less energy is required to reach the same pressure level, thus increasing the efficiency and performance of the compressor. The study also indicate, that water injection increases

possible pressure ratios from around 1.3 to approximately 1.5, although, it is also affected by the rotational frequency of the compressor (Yang et al., 2016). However, screw compressors reviewed by Ma et al. tend to reach higher compression ratios in the range of approximately $1.2 - 3$ in MVR applications (Ma et al., 2024). In addition to improving the performance of the compressor, the water injected to de-superheat the steam also serves as a lubricant which allows screw compressors to be oil-free (Yang et al., 2016).

Table 2: Volume-type steam compressors

Producer	Type	Inlet pressure	Max outlet pressure	Pressure ratio	Source
Spilling	Piston	$\approx 2\ bara$	$40\ bara$	up to 6	(HPT TCP, 2022c, Spilling, 2024a)
Kobelco	Twin screw	$1.5 - 2\ bara$	$9\ bara$	-	(HPT TCP, 2022b)
Atlas Copco	Twin screw	$0.6\ bara$	$10\ bara$	$1.8 - 6$	(Atlas Copco, n.d.–a)

One manufacturer that covers screw compressors for MVRs is the company Kobelco. Kobelco carries a twin screw compressor with water injection for de-superheating (HPT TCP, 2022b). The compressor can reach a heat supply capacity of 800 kW and a supply pressure of 8 $barg$, as presented in Table 2 (HPT TCP, 2022b). This technology is oil-free, resulting in clean steam without the risk of oil contamination, and has achieved a TRL9 (Klute et al., 2024). Another example of a supplier is Atlas Copco. Similarly to Kobelco, the Atlas Copco compressor is a twin screw compressor with water injection to improve performance, guaranteeing 100% oil-free steam (Atlas Copco, n.d.–c). The specifications for this compressor are also presented in Table 2, highlighting the large pressure ratio span, of which the lower end is in line with literature presented above. Nevertheless, according to Atlas Copco, higher pressure ratios may be achieved with multi-staged compression (Atlas Copco, n.d.–c).

To summarize, screw compressors are based on relatively simple principles and structures with minimal need for contamination since the compressors can be both lubricated and cooled down with water injections. References to manufacturers and suppliers as well as available data are limited for screw compressors for the specific use in MVR. This indicates that the technology is relatively new in this area of applications or less feasible compared to other technologies.

2.3.3 Centrifugal steam compressor

Contrary to the piston and screw compressors reviewed in previous chapters, centrifugal or turbo steam compressors are velocity-type compressors, increasing the working fluids pressure by driving up the speed of the flow. The working principle of this type of compressor is over a century old and uses a rotating impeller to guide the incoming low-pressure steam from the axis towards the perimeter of the rotor (Ma et al., 2024). The process of compressing steam in a centrifugal compressor can also be seen in Figure 13. It is evident for the applications reviewed by Ma et al. that centrifugal steam compressors are widely used both in MVR systems and within closed cycle compression heat pumps as well as other areas of applications (Ma et al., 2024). Generally, turbo compressors are preferred for systems with large volume flows and relatively small pressure lifts for optimal operation (Ma et al., 2024). The capacity to work with large flows of steam makes these compressors well suited for industrial applications, however, the limited pressure ratios can be a drawback in some situations.

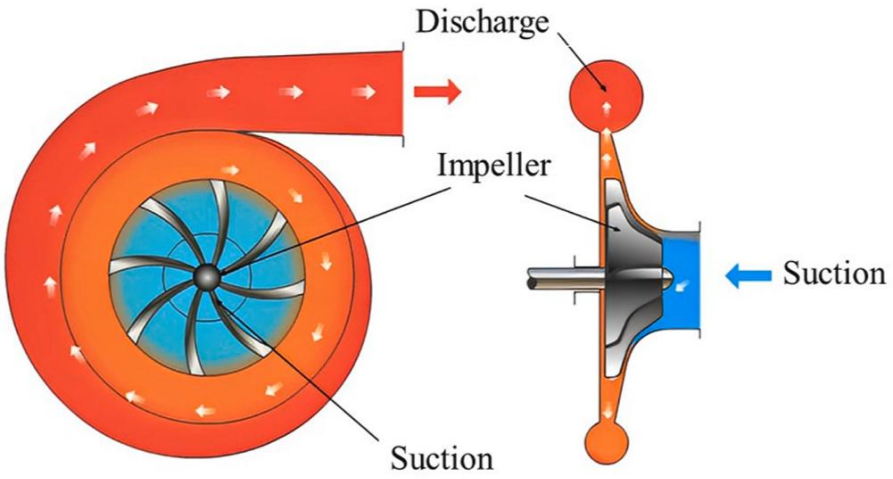

Figure 13: Working principle of centrifugal or turbo compressors (Ma et al., 2024).

Similarly to the screw compressors, centrifugal compressors also raise the temperature of the steam which moves it further from the saturation line and decreases the efficiency of the compressor. Thus, measures for lowering the discharge temperature are desired to maintain high efficiency. For centrifugal compressors Ma et al. present two solutions for reducing the temperature increase: integration with other system equipment and water injection, however, out of the two, water injection is more common in open cycle

compressors (Ma et al., 2024). Injecting water into the compressor can also improve the pressure ratio of the compression to a certain point, however, too large amounts of injected water begin to decrease it and lower the efficiency (Ma et al., 2024). While water injection can be used to improve centrifugal compression, they also require dry steam from proper operation due to sensitivity to water droplets with possible particles limited to $0.01\,mm$ (WSE Turbo, n.d.). Thus, in principle, the injected water cools down the discharge flow by evaporating, thereby absorbing energy from the steam (Ma et al., 2024).

Turbo compressors are relatively common on the MVR market with one example on a manufacturer being WSE Turbo. As can be seen in Table 3, the WSE Turbo compressor is advertised to operate with low inlet pressures and supplying steam at pressures up to 10 bar while also reaching relatively high pressure ratios (WSE Turbo, n.d.). If compared to the pressure ranges of the Kobelco screw compression, the significant difference is in the inlet pressures with the WSE Turbo also being able to work with steam under atmospheric pressure. Furthermore, the WSE Turbo compressor can take in low pressure steam at a rate of $0.3 - 3\,m^3/s$ (WSE Turbo, n.d.). The volume flow rates are dependent on the pressure of the incoming steam and mass flow ranges or limitations are not specified, making comparison difficult.

Another manufacturer is Piller with several models and sizes of centrifugal steam compressors. The three models available are VapoFan, VapoFlex, and VapoMaxX, all specialized at compressing steam at different mass flows and pressure levels (Piller, n.d.). The operation specifics for all models are presented in Table 3. Out of the three, the VapoFan 1.0 is the smallest compressor, suitable for mass flows between $0.2 - 9\,t/h$ (Piller, 2024a). The VapoFlex is a larger compressor able to take in larger mass flows up to $250\,t/h$ (Piller, 2024b). Both the VapoFan and VapoFlex, are designed to reach temperature lifts up to $11K$, which at atmospheric pressure translates to a pressure ratio of approximately 1.4. The VapoMaxX compressor, is somewhat smaller than the VapoFlex in terms of mass flow, however, it is designed to achieve greater compression with temperature lifts up to $20\,K$, or an approximate pressure ratio of 2, and supply pressures up to $20\,barg$ (Piller, 2024c). All Piller compressors can, as advertised, also be connected in series together with same type compressors to achieve larger pressure lifts.

Table 3: Speed-type centrifugal steam compressors

Producer & Models	Mass flow	Inlet pressure	Max outlet pressure	Pressure ratio	Source
WSE Turbo	-	$0.2 - 5\ bara$	$10\ bara$	up to 2.8	(WSE Turbo, n.d.)
Piller VapoFan	$0.2 - 9\ t/h$	$0.2 - 2\ bara$	-	up to ≈ 1.4	(Piller, 2024a)
VapoFlex	up to $250\ t/h$	$0.2 - 1\ bara$	$9\ bara$	up to ≈ 1.4	(Piller, 2024b)
VapoMaxX	up to $57\ t/h$	$0.4 - 2.3\ bara$	$21\ bara$	up to ≈ 2	(Piller, 2024c)

Several other manufacturers and suppliers carry similar centrifugal compressors competing with Pillar and WSE Turbo. Compared to other compressor types, centrifugal compressors benefit from being based on a reliable and old working principle while also efficiently compressing larger flows, thus making them suitable for many industrial processes. WSE Turbo also advertises that the turbo compressor is more compact with an inlet flow of $1\ m^3/s$ requiring a compressor weighing only $200\ kg$ while compressors of other technologies for similar flows weigh several tons (WSE Turbo, n.d.).

2.4 Evaporation technologies

An essential part of a steam generating heat pump is, as the name suggests, the steam generation process itself. As is evident from the different SGHP concepts presented in chapter 2.2.3 this can either be included in the closed cycle compression heat pump's heat exchanger at the heat sink side or require separate technology for the evaporation of the water. Separating the compression heat pump and the evaporation technology allows for less demands on the heat pumps as the steam generation is done separately, however, this also leads to a slight decrease in the maximum supply temperatures of these SGHPs (Klute et al., 2024). There are two main principles on which the evaporation technologies can be based: flash evaporation or "normal" evaporation. Following paragraphs will describe the different technologies available for steam generation based on these two principles.

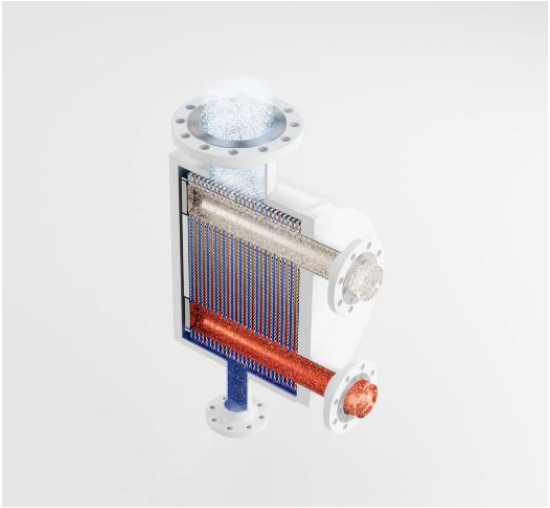

Figure 14: Illustration of the operation in a Vahterus evaporator (Vahterus Oy, n.d.).

Normal evaporation refers to steam generation in an evaporator in which heat is added to a stream of water, thus evaporating it at a constant pressure. The term normal is used here since evaporating or boiling water is the most basic and everyday manner to change the phase of water from liquid to vapor. The evaporator is similar to a heat exchanger in that the water stream to be evaporated and the hot water coming from the compression heat pump does not mix but rather only heat is transferred from one stream to the other. One example is the evaporators by Vahterus (Vahterus Oy, n.d.). In these the feed water enters the evaporator through the bottom while the hot water enters through the side panel to then circulate through the plates transferring the heat. The feed water boils as the heat is transferred to it and flows out of the evaporator from the top. Depending on the design of the evaporator the steam supplied from the evaporator can either be wet, meaning it still contains liquid water, or saturated and dry. An evaporator supplying wet steam is portrayed in Figure 14. Especially in the case of wet steam an additional separator is required to ensure dry saturated steam is fed into the steam system. In some applications an evaporator may also be referred to as a reboiler, if recently condensed water is re-evaporated.

Flash evaporation, on the other hand, occurs when the pressure drops suddenly which triggers the evaporation (Wang et al., 2019). Given that the boiling point of water is dependent on its pressure, with lower pressures also lowering the evaporation temperature, a sufficiently large and sudden pressure drop will cause the liquid water to shortly exist at a pressure and temperature level at which it should be steam. This results in the water quickly vaporizing to reach a stable state, or flashing. Flash evaporation takes place in equipment usually referred to as flash tanks or flash vessels. Contrary to evaporators, the feedwater entering the flash vessel is usually fed directly from the heat pump to evaporate (Klute et al., 2024). This means that there

is no closed loop of hot water circulating between the heat pump and flash vessel. The connection can, however, be realized in different ways with the two main options illustrated in Figure 15. In the first alternative the hot feed water, which may also be pressurized, enters the flash vessel through a throttle, thus evaporating as presented in Figure 15a). In the second, the condensate from the flash vessel is separately circulated through a heat pump and subsequently flashed as the water returns to the vessel according to Figure 15b). Additionally, flash vessels can operate either above or under atmospheric pressure, for example, depending on the feed water conditions, especially in a flash vessel of the first type. If the stream of fluid entering the flash vessel is pressurized, the operating pressure of the vessel can remain at or even above atmospheric pressure. If the fluid entering is at or around 1 *bara*, flashing it would require the pressure to drop significantly under atmospheric pressure.

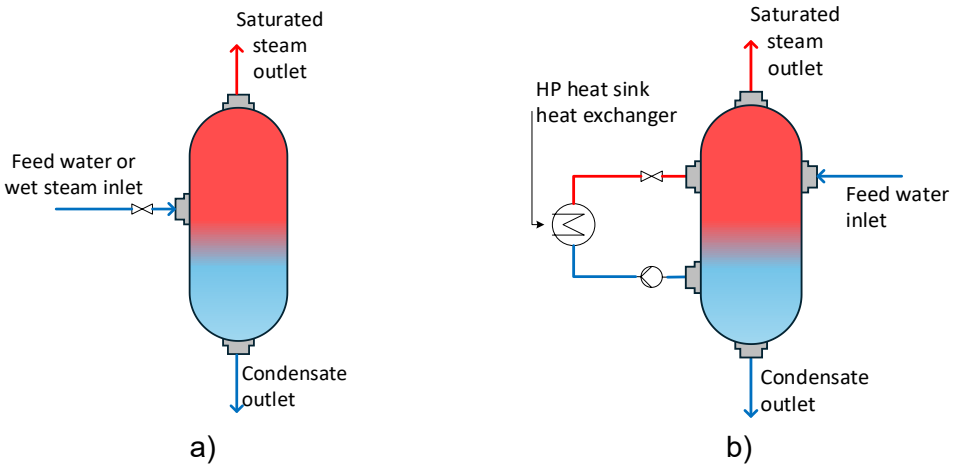

Figure 15: Simplified sketches of a) a flash vessels without an integrated loop connected to a heat pump (Goodarzvand-Chegini et al., 2023) and b) one with an integrated heat pump (Jouni et al., 2024).

Based on available literature, most flash vessel systems presented build on the first concept with the feed water itself being flashed to generate steam. One such system presented is reviewing single and double flashing of pressurized geothermal hot water for power production (Zeyghami, 2010). In the case of double flashing, the condensate leaving the first flash vessel is directed into a second vessel as input where the pressure drops further to generate lower pressure steam. Another article carried out a case study on flash vessels for utility steam generation from return condensate in a gas refinery (Goodarzvand-Chegini et al., 2023). In this case two possibilities for upgrading the obtained low pressure flash steam were reviewed: mechanically pressurizing the steam with MVRs and utilizing high pressure steam from the

boiler to upgrade the flash steam in a TVR. While these examples highlight the interest in the first concept, the latter is also regarded in some papers. One example is the study made by Jouni et al. evaluating a flash vessel in combination with a compression heat pump as well as MVRs (Jouni et al., 2024). The system in this study, also presented in Figure 16, consists of a vapor compression heat pump with a synthetic refrigerant, a flash vessel with a forced circulation to the reboiler, and two steam compressors with a de-superheater in between that utilizes condensation from the flash vessel. As a result of the study Jouni et al. found that the flash tank in connection to a heat pump and MVR is a an important part of equipment for industrial applications with high flexibility and robustness (Jouni et al., 2024).

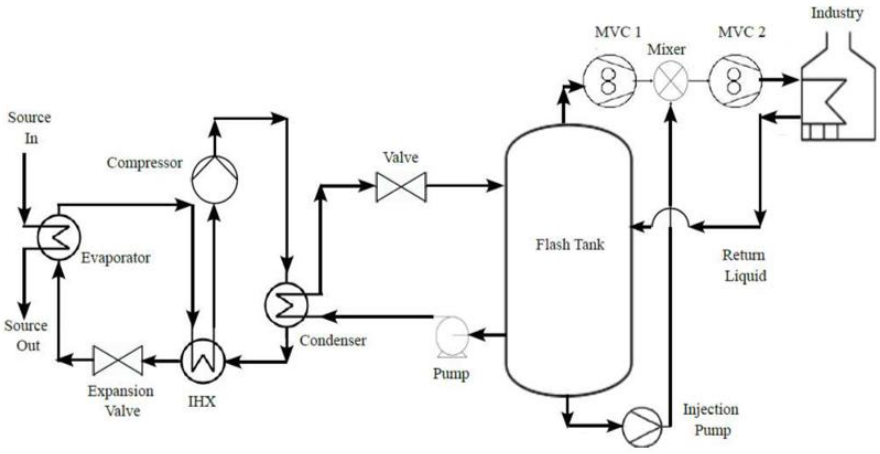

Figure 16: The steam generation system studied by Jouni et al as presented in the report (Jouni et al., 2024).

Steam accumulators are, additionally, somewhat related to the flash vessel technology in that they also rely on pressure drops to produce steam (Spirax Sarco, n.d.). Nevertheless, given that their main purpose is not to produce steam but rather to regenerate steam that has been liquified for better storage, they are not further considered.

3 Methodology

As the purpose of this thesis is to examine steam generating heat pumps and their adaption in industry, several solutions are compared. For different solutions and their performance to be fairly evaluated and compared to each other, they need to be integrated into a system and context. In the case of steam generation systems and steam generating heat pumps, the logical context is an industrial process and steam cycle. As presented in the literature review, flash vessels as well as closed cycle compression heat pumps supplying steam are regarded in studies and by several suppliers. Nevertheless, the combination of HTHP and MVR are more rarely reviewed in the context of industrial steam generation. Therefore, this thesis focuses on examining configurations of HTHP or VHTHP, steam separators and compressors to assess the impact of design choices on the efficiency. The solutions are examined in two different processes of different steam consumptions levels, one with a lower power level as well as one with a higher power level.

All calculations performed in this thesis are based on the XSteam-library available as an add-on in MATLAB as well as its equivalent in Excel (Holmgren, 2007). In addition to MATLAB and Excel, Microsoft Visio is utilized for illustrations of the various processes and steam cycles. The reference processes are presented further in chapter 3.1 with the subsections 3.1.1 and 3.1.2 dedicated to the low power steam demand of 800 kW and high power steam demand of 20 MW, respectively. Chapter 3.2 dictates the basis for the steam generation designs, including values and equations used. In chapter 3.3 the methodology for evaluating the possible SGHP solutions is presented along with the Key Performance Indicators (KPI). Finally, a financial perspective is defined in chapter 3.4.

3.1 Industrial reference processes

The processes chosen for the study in this thesis are based on existing industrial plants. However, due to confidentiality they cannot be presented and utilized in their actual structure. Therefore, reference processes are created to represent these plants although simplified and generalized to maintain anonymity. Pressure levels of the required steam conditions as well as the power level of the steam consumption are generalized, and the consumption target is not specified as this is assumed not to affect the steam supply contexts. Condensates and other waterflows returning from the consumption target are, however, assumed to not be contaminated nor in need of extra attention prior to circling back to the steam generator. The reference processes considered consist of a fossil fuel boiler, a feed water system, and a steam consumer. A fossil fuel boiler was chosen to be able to examine the

reductions in CO_2 emissions that steam generating heat pumps can entail, since the main motive for electrifying industrial processes is to replace fossil fuels.

The reference processes that act as context and a basis for potential solutions are illustrated in Visio. The flow diagrams of these processes only cover streams essential for the integration of steam generating heat pumps. The flow diagrams do not include all safety valves or similar instruments but rather highlight the overall context of a process. Similar flow diagrams are also presented for all potential solutions examined in this thesis. In the case of potential solutions, which will replace the solutions within the revision boundaries of the reference processes, the flow diagrams are more exact and contain more detail, however, they still do not cover all safety valves etc. Technology selections for applications into the reference processes are based mainly, however, not exclusively, on the literature review and technologies evaluated there. Each flow diagram presented also contains defined and numbered points in which the fluid conditions are specified for calculation purposes. In connection to these, tables are used to structurally present the temperature, pressure, enthalpy etc. at each defined point.

3.1.1 Low power steam demand

The reference industrial process with low power steam demand assumes a consumer requiring 800 kW of steam at steady consumption and is depicted in a flow diagram in Figure 17. The detailed steam requirements along with other values used are listed in Table 4. These steam requirements result in a steam mass flow of just over one ton per hour to the consumer. The assumed condensate return rate of 100% means no condensate losses are accounted for requiring make-up water. Similarly, blow down is not considered, although this would take place in a feed water tank. These assumptions are seen to not affect the adaptation of steam generating heat pumps as they take place outside the scope, and are therefore made to simplify the calculations etc.

Table 4: Process values for low power steam demand.

Aspect	Value	Source, if applicable
Steam		
Demand	800 kW	
Pressure	6 $barg$, saturated vapor	
Mass flow	0.33 $kg/s \approx 1.2\ t/h$	
Condensate		
Pressure and Temp.	0 $barg, 80\ °C$	
Return rate	100 %	
Feed water		
Temperature	120 $°C$, saturated liquid	
Boiler		
Fuel	Light Fuel Oil (LFO)	
LHV	43.0 GJ/t	(Alakangas et al., 2016)
Emission factor	73.5 $t\ CO_2/TJ$	(Alakangas et al., 2016)
Efficiency	85 %	(Atlas Copco, n.d.–b)
Waste heat (water)		
Available Temp.	65 $°C$	
Return Temp.	55 $°C$	
Mass flow	not limited, covers full demand	
Pump		(Hofmann and Tsatsa-ronis, 2015)
Efficiency	$\eta_{is} = 0.84$	
Operation		
Annual hours	8000 h	
Fuel consumption	941 $kW = 79\ kg/h$	
CO_2 emissions	1990 $t\ CO_2/year$	

Based on the conditions specified in the previous paragraph together with the isentropic efficiency of the feed water pump, the fluid properties can be calculated for each numbered point in the process. The calculated values are presented in Table 5. Further calculations regarding fuel consumption and emissions, however, require additional information on fuel properties and boiler efficiencies. The efficiency of an LFO boiler is based on average efficiencies of fuel boilers. Given that fuel consumption is only indicative for the comparison of systems with different heat pump solutions, this level of accuracy is deemed sufficient. Based on this efficiency, fuel consumption can also be calculated and further used to determine the CO_2 emissions one year of operations would entail. The oil consumption rate as well as the annual emissions are presented in Table 4.

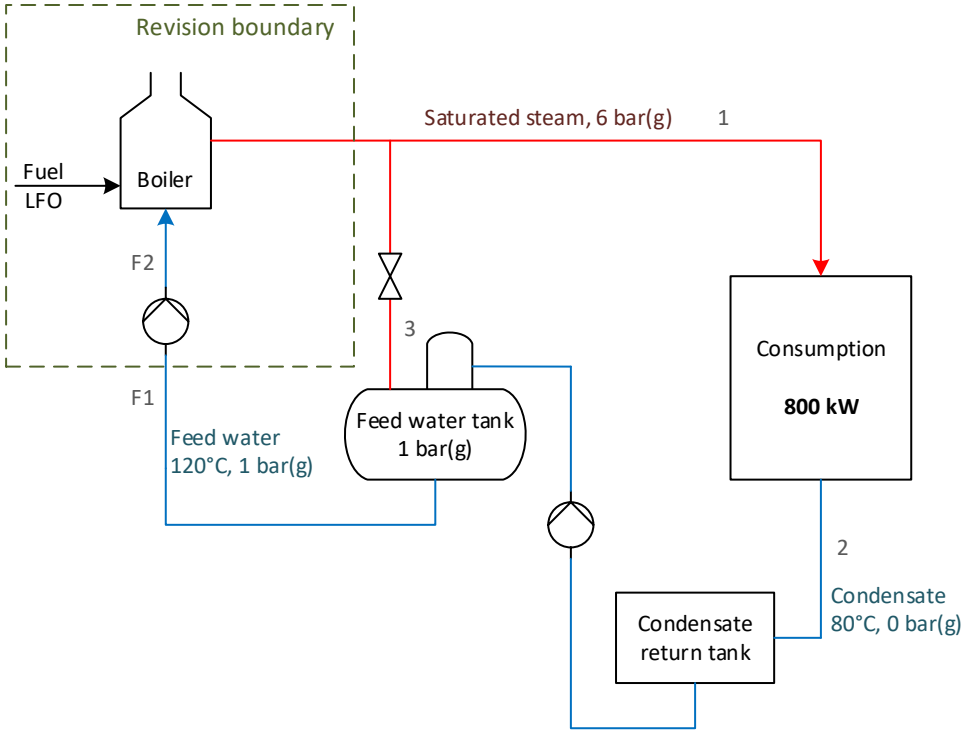

Figure 17: Flow diagram of industrial reference process with low power steam demand.

Table 5: Fluid conditions at each process point in Figure 17.

Process points	Pressure	Temp.	Enthalpy	Entropy	Steam fraction	Mass flow
1	7 $bara$	165 $°C$	2762.7 kJ/kg	6.71 $kJ/kg°C$	1	0.33 kg/s
2	1 $bara$	80 $°C$	335.0 kJ/kg	1.08 $kJ/kg°C$		0.33 kg/s
3	2 $bara$	147 $°C$	2762.7 kJ/kg	7.27 $kJ/kg°C$		0.02 kg/s
F1	2 $bara$	120 $°C$	503.8 kJ/kg	1.53 $kJ/kg°C$	0	0.35 kg/s
F2	7 $bara$	120 $°C$	504.4 kJ/kg	1.53 $kJ/kg°C$		0.35 kg/s

3.1.2 High power steam demand

The high power reference process has a steam demand significantly higher than that of the low power scenario, requiring $20MW$ of saturated steam with a steady consumption, as per the flow diagram presented in Figure 18. The process values used for this process, including steam requirements, are presented in Table 6. This power and pressure level equates to a steam mass flow of $\approx 30t/h$ going to the consumer. Similarly to the low power scenario, blow down and mass losses in the condensate are not accounted for to simplify calculations not directly affecting the integration of steam generating heat pumps.

Table 6: Process values for high power steam demand.

Aspect	Value	Source, if applicable
Steam		
Demand	20 MW	
Pressure	3 $barg$, saturated vapor	
Mass flow	8.32 $kg/s \approx 30\ t/h$	
Condensate		
Pressure and Temp.	0 $barg, 80\ °C$	
Return rate	100 %	
Feed water		
Temperature	120 $°C$, saturated liquid	
Boiler		
Fuel	Natural Gas (NG)	
LHV	36 MJ/m^3	(Alakangas et al., 2016)
Emission factor	55.04 $t\ CO_2\ /TJ$	(Alakangas et al., 2016)
Efficiency	80 %	(Atlas Copco, n.d.–b)
Waste heat (water)		
Available Temp.	75 $°C$	
Return Temp.	55 $°C$	
Mass flow	not limited, covers full demand	
Pump		(Hofmann and Tsatsa-
Efficiency	$\eta_{is} = 0.84$	ronis, 2015)
Operation		
Annual hours	8000 h	
Fuel consumption	25 $MW = 2500\ m^3/h$	
CO_2 emissions	39 600 $t\ CO_2/year$	

Based on these specifications, the fluid conditions are calculated for each point in the process and presented in Table 7. For the following fuel consumption calculations the boiler efficiency is based on average efficiencies similarly to the previous scenario, however, taking into account that gas boilers generally have a lower fuel-to-steam efficiency compared to oil boilers (Atlas Copco, n.d.–b). Based on this, as well as the fuel properties of natural gas, which especially in terms of the emission factor differs from LFO, the fuel consumption rate and annual emissions can be calculated. The obtained values are consumption and emissions are presented in Table 6.

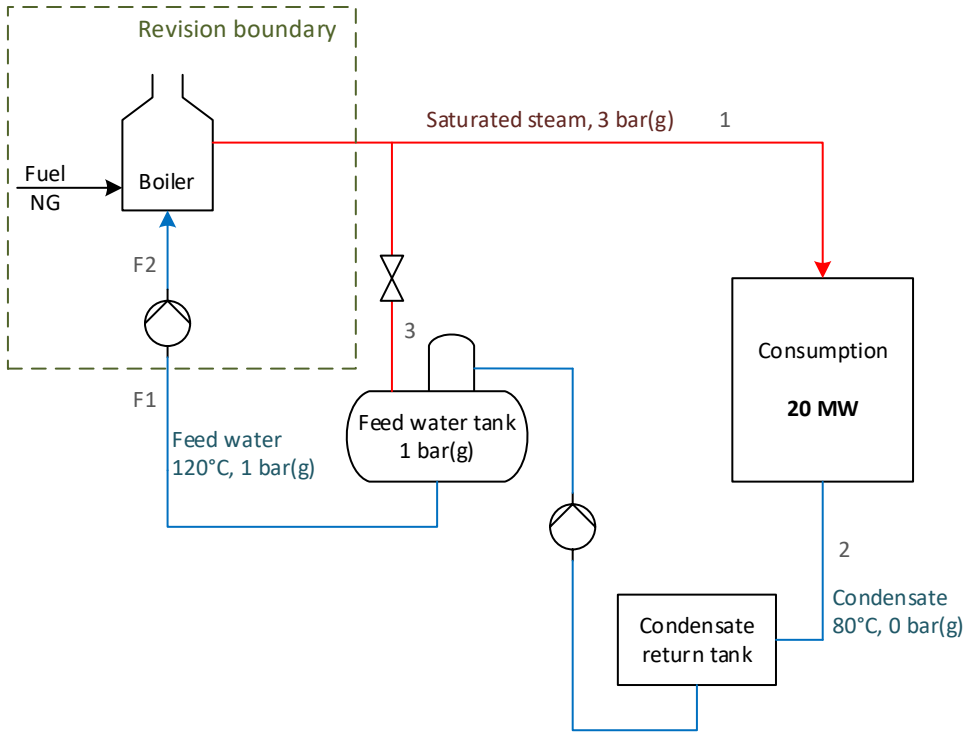

Figure 18: Flow diagram of industrial reference process with high power steam demand.

Table 7: Fluid conditions at each process point in Figure 18.

Process points	Pressure	Temp.	Enthalpy	Entropy	Steam fraction	Mass flow
1	4 *bara*	144 °C	2738.1 kJ/kg	6.90 $kJ/kg°C$	1	8.32 kg/s
2	1 *bara*	80 °C	335.0 kJ/kg	1.08 $kJ/kg°C$		8.32 kg/s
3	2 *bara*	135 °C	2738.1 kJ/kg	7.21 $kJ/kg°C$		0.63 kg/s
F1	2 *bara*	120 °C	503.8 kJ/kg	1.53 $kJ/kg°C$	0	8.95 kg/s
F2	4 *bara*	120 °C	504.0 kJ/kg	1.53 $kJ/kg°C$		8.95 kg/s

3.2 SGHP Solutions

The objective of the developed SGHP solutions evaluated in this thesis is to replace the fossil-based steam production within the revision boundaries depicted in Figure 17 and Figure 18. The solutions, which are further presented in chapter 4, are designed using four main categories of equipment: closed cycle heat pumps, a steam separator, steam compressors, and pumps. For the purpose of performance calculations, suppliers and products reviewed in the literature review are chosen to represent some of the different options of technology and get operational specifics and limitations. The closed cycle heat pump used in calculations is the HeatBooster by Heaten.

Similarly, piston, screw and turbo compressors are represented by the Spilling, Atlas Copco, and Piller VapoMaxX MVRs, respectively. For the pumps, no specific supplier is referenced, but rather, efficiencies are assumed based literature and general averages. Finally, steam separators are considered solely through mass and energy balances, assuming no losses occur in the separation process. A list of all parameters used in the design and performance calculations can be found presented in Table 8. Additionally, all demand and availability assumptions presented in connection to the reference processes apply.

Table 8: Design basis specifications and parameters

Equipment / Aspect	Limitations / parameter	Source
Heaten, HeatBooster		
Capacity	$800 - 2500\ kW$	(Heaten, n.d.–a)
Hot water supply	$90 - 200°C$	(Heaten, n.d.–a)
Direct steam supply	up to $180°C$ / $10\ bar(a)$	(Heaten, n.d.–a)
HEX ΔT	$5\ K$	
HEX pressure loss	$0.7\ bar$	
% of Carnot COP	≈ 50 %	(Heaten, 2026)
Max Temp. Lift	$80\ K$	(Heaten, 2026)
Spilling		
Min inlet pressure	$2\ bar(a)$	(Spilling, 2024b)
Max supply pressure	$\approx 60\ bar(a)$	(Spilling, 2024b)
Pressure ratio	up to 3 per stage	(HPT TCP, 2022c)
Steam mass flow	$\approx 1 - 20\ t/h$	(Spilling, 2024b)
η_{is}	85 %	
η	70 %	
Atlas Copco		
Min inlet pressure	$0.6\ bar(a)$	(Atlas Copco, n.d.–a)
Max supply pressure	$10 - 14\ bar(a)$	(Atlas Copco, n.d.–a)
Pressure ratio	$1.8 - 6$	(Atlas Copco, n.d.–a)
Steam mass flow	up to $\approx 2 - 6\ t/h$ (at $0.7 - 1.5\ bar(a)$ inlet)	(Atlas Copco, n.d.–a)
η_{is}	75 %	(He et al., 2012)
η	85 %	
Piller, VapoMaxX		
Min inlet pressure	$\approx 0.4\ bar(a)$	(Piller, 2024c)
Max supply pressure	$21\ bar(a)$	(Piller, 2024c)
Pressure ratio	up to ≈ 2 / $(20K)$	(Piller, 2024c)
Steam mass flow	up to $57\ t/h$	(Piller, 2024c)
η_{is}	73 %	(Son et al., 2021)
η	87 %	(Piller, 2024c)
Pumps		
η_{is}	84 %	(Hofmann and Tsatsaronis, 2015)
η	75 %	

In the case of some efficiencies, including the isentropic and total efficiency of the Spilling compressor as well as the total efficiency of the Atlas Copco screw compressor, credible values could not be found in literature. Therefore, the efficiency values used are experience-based assumptions for similar technology. Additionally, the isentropic efficiencies for the screw and centrifugal compressors are not supplier-specific but assumed to be of sufficient accuracy, since they are mainly dependent on the technology rather than design specifics of the type of compressor. Given these specifications, several solutions of heat pump and MVR configurations are developed and simulated in Excel. For each steam power level different pressure levels are tested for the steam separation process to evaluate the balance between the temperature lift of the closed cycle heat pump and the pressure increase required by MVR technology. The pressure levels are chosen based on a low- and high-end extreme with the minimum supply temperature of the HeatBooster setting the low-end extreme at 0.7 $bar(a)$ and the steam supply pressure of each reference process dictating the high-end extreme.

The different scenarios are, as mentioned, simulated in excel using XSteam to aid calculations. The pump electrical power is obtained by multiplying the enthalpy lift by the mass flow and dividing that by the pump overall efficiency, as per equation (1). Similarly, the power required by the steam compressors are calculated by first finding the real enthalpy reached after the compression stage and then utilizing that in combination with the mass flow and overall efficiency to obtain the electric power consumption. These calculations are based on equations (2) and (3), respectively.

$$P_{el,pump} = \frac{\Delta h \cdot \dot{m}}{\eta} = 100 \frac{v_{before} \cdot \Delta p \cdot \dot{m}}{\eta_{is} \cdot \eta} \tag{1}$$

$$h_{real} = \frac{h_{ideal} - h_{before}}{\eta_{is}} + h_{before} \tag{2}$$

$$P_{el,comp} = \frac{\left(h_{real} - h_{before}\right) \cdot \dot{m}}{\eta} \tag{3}$$

The variables in these equations for the electrical powers P_{el} are the enthalpy h, pressure p, steam or water mass flow $\dot{m}$, specific volume of the fluid v, isentropic efficiency η_{is}, and total efficiency η. As opposed to the pumps and compressors, the electric power consumption of the compressor heat pump is based on the temperature difference rather than enthalpy difference. The calculation of the ideal Carnot COP of a compression heat pump is presented in equation (4). Based on the real COP of the HeatBooster being 50%

of the ideal COP, the electric power consumption of the heat pump can be calculated using equation (5).

$$COP_{carnot} = \frac{T_H}{T_H - T_C} = \frac{T_{supply} + \Delta T_{HEX}}{T_{supply} + \Delta T_{HEX} - \left(T_{waste,return} - \Delta T_{HEX}\right)} \quad (4)$$

$$P_{el,HP} = \frac{P_{supply}}{COP_{carnot} \cdot 50\%} \quad (5)$$

When calculating the Carnot COP, both the condensation and evaporation temperatures of the heat pump, T_H and T_C need to be in kelvin. To obtain the temperatures within the heat pump, the $5K$ pinch temperature difference in both heat exchangers is added to the supply and returning temperatures. Furthermore, the power consumed by the heat pump is calculated by dividing the heat power it supplies by the Carnot COP multiplied by the 50%, which is specified by the supplier. In addition to the electrical powers, the amount of condensate needed to de-superheat the compressed steam as it comes out of the compressors is also calculated. This is done through the energy and mass balances which creates the system of equations (6) with the flows of the superheated steam and saturated water mixing to result in saturated steam.

$$\begin{cases} \dot{m}_{steam} \cdot h_{steam} + \dot{m}_{water} \cdot h_{water} = \dot{m}_{sat.\ steam} \cdot h_{sat.\ steam} \\ \dot{m}_{steam} + \dot{m}_{water} = \dot{m}_{sat.\ steam} \end{cases} \quad (6)$$

The energy balance is calculated using the mass flows of steam and water $\dot{m}$ and enthalpy of the streams h. The results of the calculations and Excel simulations presented above, at each numbered point of the processes, are collected in a table for each solution and flow diagram, similarly to the reference process presentations. In the case of SGHP solutions, however, illustrations and tables are additionally accompanied by a log p-h diagram to further help visualize the process. The results of the Excel models are then also used as the basis for calculating process performance indicators etc., which are further elaborated on in the following chapter 3.3.

3.3 Process Key Performance Indicators

To be able to fairly and consistently evaluate several solutions, numerical key performance indicators (KPI) need to be developed and established. The operation of heat pumps is most commonly defined by a coefficient of performance (COP). Therefore, the COP will also serve as the main KPI for the steam generating heat pump solutions developed in this thesis. Given that these heat pump solutions strive to replace the boiler and supply the entire steam demand, scope 1 carbon dioxide reduction will not be a relevant KPI itself, nevertheless, if scope 2 emissions, referring to emissions from the production of the electricity consumed, are taken into account, the relative abatement becomes an indicator for the location dependency of the solution's feasibility. Therefore, decrease in total emissions as a percentage of the reference process acts as the second KPI. An analysis of the KPIs is then done to evaluate the relevance of the solutions developed in actual industrial cases and possible bottlenecks and drawbacks. Calculations and assumptions used in obtaining the KPIs are further defined in following paragraphs.

The coefficient of performance is essentially calculated as the useful energy output over the input energy in terms of electricity consumed by the pumps and compressors. Here, the electricity consumed by the pump located between the condensate tank and the feed water tank, in both the reference processes as well as the solutions, is not accounted for in the input energy as it is not included within the revision boundary, thus assumed to be equal in all scenarios, therefore not having a significant impact on the comparison of COPs. In the case of steam generating heat pumps, and the solutions developed in this thesis, the useful energy is the steam supplied to the consumer, as per (7). The calculations of the COP values are done in connection to the Excel models of the solutions and finally presented in graphs. Given that some aspects of the assumptions being the models are subject to uncertainty, a simple sensitivity analysis is performed as well.

$$COP = \frac{Q_{useful}}{W_{el}} = \frac{Q_{demand}}{W_{pumps} + W_{compressors}} \tag{7}$$

Based on the results of the comparison of solutions from the perspective of the COP, one or two solutions per reference process are identified as technological recommendations. These recommended solutions are then further evaluated based on their potential for CO_2 abatement. The total emission reduction of scopes 1 and 2 is done for four separate scenarios. In the first scenario the electricity used is assumed to be fully renewable, which equates to only accounting for scope 1 emissions. In the three following scenarios scope 2 emissions are also included, for heat pumps operating in Finland, Sweden,

and within EU. The carbon intensities used are production averages from 2024 at 37 gCO_2e/kWh, 7 gCO_2e/kWh, and 187 gCO_2e/kWh for Finland, Sweden, and EU27, respectively (EEA, 2025). Comparing the electricity mix on which the heat pump operates, and the subsequent relative abatement, will provide insight into the relevance of the fuel type and location on the feasibility of the heat pump solution.

The process KPIs obtained in the calculations are analyzed both independently for the two processes and power levels to evaluate the applicability and relevance of that specific solution and set up. The KPIs are, however, also compared and analyzed between the two processes to examine the effect that the size of the process has on the heat pump solution selection.

3.4 Financial perspective

Alongside the technical evaluation of the different SGHP solutions, an additional financial perspective is also reviewed to provide an economic aspect to the feasibility of the solutions in industry. The financials of each solution are based on the annual savings in operational costs that the heat pumps generate. In this thesis, the annual savings consider the reduction in fuel costs as the fossil fuel boilers are phased out as well as the added electricity costs of electricity consumed by the heat pump solution. Other operational costs including maintenance and possible CO_2 emission allowances under the EU ETS are excluded from the financial calculations as they require more detailed system design etc. to be able to estimate at a level of sufficient accuracy. Since fuel and electricity prices vary depending on location and national taxation, the financial evaluation is done separately for Finland and Sweden, as well as for the EU average prices for comparison. In all three cases the prices used are averages of the years $2023 - 2025$ to base the calculations on the market situations after the energy crisis of 2022.

In the Finnish scenarios all prices are three-year averages calculated based on data from the Statistics Finland. The average price for light fuel oil over this time in Finland was 1.35 €/l or 1.49 €/kg (Tilastokeskus, 2026b). However, since these are consumer prices a VAT of 25.5% is subtracted from it to obtain the fuel price for industrial customers. This results in an LFO-price of 1.19 €/kg. In the case of natural gas, the average price for a customer with annual consumption of $27\,778 - 277\,777$ MWh is 66.79 €/MWh (Tilastokeskus, 2026a). However, since the natural gas price excludes all taxes, these need to be added separately. According to the Finnish Tax Administration, taxes on natural gas include energy content tax, carbon dioxide tax, and a strategic stockpile fee, which in 2026 amounts to a total of 23.37 €/MWh (Verohallinto, 2026). Finally, the statistics of the Finnish electricity price from this three-year period are, similarly to the natural gas, available for

several consumption levels. Based on the annual consumptions of the heat pumps for the 800 kW and 20MW processes, the two would fall into different categories of enterprise and corporate clients with annual consumptions between $2\,000 - 19\,999\ MWh$ and $20\,000 - 69\,999\ MWh$, respectively. However, for the solutions of both power level contexts, the higher range prices are used since it can be assumed that the smaller process is connected to a larger industrial plant or customer raising the total annual consumption to that category. Based on this the electricity price used in the financial calculations is 61.05 €/MWh (Tilastokeskus, 2026b).

For Sweden, the natural gas and electricity prices are based on data from Statistics Sweden, while the LFO price is based on the statistics database by the Swedish Energy Agency. The data on LFO prices are available for two types of oils, with and without SO_2, however, excluding data from 2025. Since the LFO in this study is used in a small boiler in which the latter is more commonly used, calculations also assume that fuel oil without sulphur dioxide is used. Based on this the $2023 - 2024$ average total price for LFO, including energy and carbon dioxide taxes, amounts to $1\,217.50\ SEK/MWh$ (Energimyndigheten, 2025). Similarly to the Finnish price, the cost of natural gas in Sweden is also dependent on annual total consumption. With a consumption of $30\,000 - 299\,999\ MWh$ per year, the average three-year natural gas price for an industrial customer in Sweden amounts to $1\,211.88\ SEK/MWh$ (Statistikmyndigheten, 2026b). Lastly, the average electricity in Sweden is based on the same annual consumption category as in Finland of $20\,000 - 69\,999\ MWh$. For electricity consumption for direct use in production processes, therefore only including a 0.6 $öre/kWh$ tax, the three-year average total price of 820.97 SEK/MWh (Statistikmyndigheten, 2026a). This statistic does not, however, account for differences in electricity prices over the four Swedish bidding zones. In order for the Swedish prices to be comparable a coefficient of 10.9 $SEK/€$ is used to obtain the costs in euros.

To compare the fuel and electricity prices in Finland and Sweden, and subsequently the feasibility of the solutions in different locations, averages for the area of the European Union are also calculated. The price statistics for LFO, or heating gas oil as it is also referred to, in the EU are available in a weekly oil bulletin provided by the European commission. Based on this, the average price, including taxes, for the period of $2023 - 2025$ is 1.09 €/l or 1.13 €/kg (European Commission, 2026). When compared to the averages in Finland, it is relatively close to the price including all taxes but the VAT. As for the price data for natural gas and electricity, it is available in datasets maintained by Eurostat. The natural gas average price over the years $2023 - 2024$ for non-household consumers is 49.15 €/MWh (Eurostat, 2026b). Similarly, the average price for electricity in the EU27 area for non-household consumers over the over the years 2023, 2024, and the first half of 2025 is 197.64 €/MWh, including taxes other than VAT (Eurostat, 2026a). With the

natural gas price in the EU being significantly lower than that of Finland and Sweden, while the electricity is more than two times more expensive, the economic feasibility calculations will be greatly affected by the chosen location, especially in the case of the solutions for the larger reference process.

Table 9: Average fuel and electricity prices in Finland, Sweden and the EU

Energy source	FIN	SWE	EU27
Light Fuel Oil	99.40 €/MWh	111.70 €/MWh	94.60 €/MWh
Natural Gas	90.16 €/MWh	111.18 €/MWh	49.15 €/MWh
Electricity	61.05 €/MWh	75.32 €/MWh	197.64 €/MWh

The national and EU average prices presented above are compiled in Table 9. These values are used in calculating the annual savings according to equations (8) and (9) for the 800 kW and 20 MW processes, respectively. Based on the savings, a limit for available investment capital is then calculated using a desired payback time constant. In this thesis, a payback time of 6 years is used to obtain a maximum CAPEX for the solution according to equation (10).

$$savings/year = Q_{LFO} \cdot c_{LFO} - \frac{800\ kW \cdot 8000\ h}{COP \cdot 1000} \cdot c_{el} \tag{8}$$

$$savings/year = Q_{NG} \cdot c_{NG} - \frac{20\ MW \cdot 8000\ h}{COP} \cdot c_{el} \tag{9}$$

$$CAPEX = 6\ years \cdot savings/year \tag{10}$$

The equations above include fuel consumption in terms of energy Q as well as the specific cost of fuel or electricity c in terms of €/MWh.

4 Results

Based on the equipment selection presented in chapter 3.2, several solutions are developed to replace fossil steam production in the industrial reference processes with heat pump-based steam generation systems. For both reference processes, three example solutions are presented in chapters 4.1 and 4.2 respectively, to illustrate the effect of the steam separation pressure on the configuration of technologies and design choices. Each chapter is then concluded with a graphical presentation of the obtained COPs of 4-7 balance scenarios in addition to the three designs presented in more detail. Furthermore, the CO_2 abatement calculations for the recommended solutions are also presented here.

In chapter 4.3 a financial perspective is given to the technological KPIs. The annual savings and investment cost estimation is done for the recommended solutions, however, the range is also presented for all solutions evaluated. Finally, the results from both the technological and financial perspectives are summarized and discussed in chapter 4.4 to give an overall view of the suggestions of all obtained KPIs and calculation results.

4.1 Low power steam demand

For the low power steam demand reference process, with a steam requirement of 800 kW at 6 $bar(g)$, the three example solutions chosen are designed around steam separation pressures of 0.7 $bar(a)$, which simultaneously demonstrates a system with steam separation below the pressure of the feedwater tank as well as the lower end extreme scenario, 3.4 $bar(a)$, representing a scenario where the steam separation occurs above the pressure of the feedwater tank, and 7 $bar(a)$, at which the steam is directly produced at the required pressure and no MVRs are subsequently required. Given that this process has a higher steam pressure demand for the steam while the low power equates to a relatively low mass flow, the equipment selected for these solutions include the HeatBooster, the piston compressor by Spilling and screw compressor by Atlas Copco.

The first solution, in which the steam separation occurs at 0.7 $bar(a)$ or $-$ 0.3 $bar(g)$, can be found illustrated in Figure 19. The solution consists of a HeatBooster compression heat pump, a steam separation vessel, a screw compressor, and a two-stage piston compressor. Since the separator pressure is lower than the pressure of the feed water tank, the water is throttled which causes a small amount of the flow to flash as a result of the pressure drop. However, in this scenario, only approximately 6% of the mass flow evaporates due to the flashing. The water circulated from the separator to the closed heat pump is driven by a pump, which covers the pressure loss at the

heat exchanger of 0.7 bar. Additionally, it is specified that half of the mass flow passing through the heat exchanger or steam generator is evaporated. This is to make the model applicable also in the scenario that the heat pump heat exchanger itself cannot produce steam, but a separate evaporator heat exchanger is required in between. The saturated steam exiting the steam separator at 0.7 $bar(a)$ and 90°C is first lead to the screw compressor where it is pressurized to 2 $bar(a)$. The outlet pressure of 2 bar is motivated by the minimum inlet pressure of the following piston compressor, in which the steam is then compressed to the required 7 $bar(a)$ in two stages. Between each stage of compression, the steam flow is de-superheated, using condensate from the bottom of the steam separator. The condensate is pumped to the final steam pressure and later throttled to match the steam pressure at each injection point. This SGHP solution requires a waste heat mass flow of 11.3 kg/s or ≈ 41 t/h.

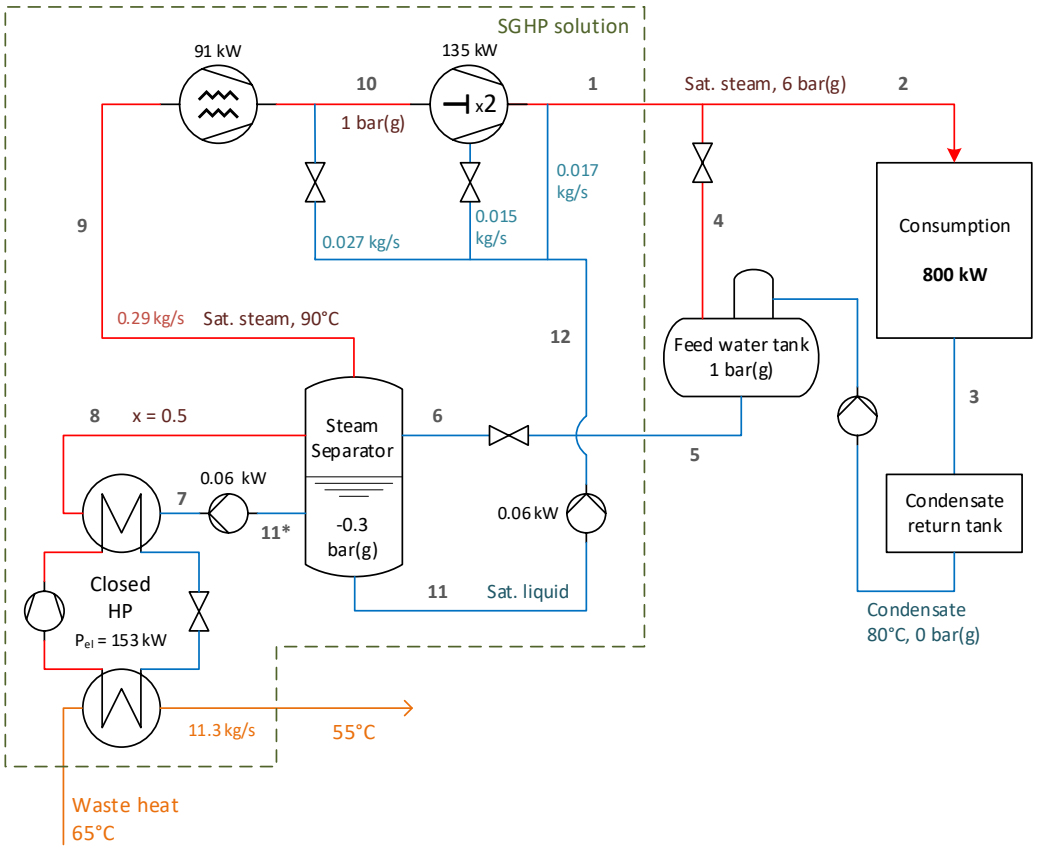

Figure 19: Flow diagram for the SGHP solution with steam separation at 0.7 bar(a) and 800kW steam production.

Table 10: Fluid conditions at each process point in Figure 19.

Process points	Pressure	Temp.	Enthalpy	Entropy	Steam fraction	Mass flow
1	7 *bara*	165 °C	2763 kJ/kg	6.71 $kJ/kg°C$	1	0.35 kg/s
2	7 *bara*	165 °C	2763 kJ/kg	6.71 $kJ/kg°C$	1	0.33 kg/s
3	1 *bara*	80 °C	335 kJ/kg	1.08 $kJ/kg°C$		0.33 kg/s
4	2 *bara*	147 °C	2763 kJ/kg	7.27 $kJ/kg°C$		0.02 kg/s
5	2 *bara*	120 °C	505 kJ/kg	1.53 $kJ/kg°C$	0	0.35 kg/s
6	0.7 *bara*	90 °C	505 kJ/kg	1.54 $kJ/kg°C$	0.06	0.35 kg/s
7	1.4 *bara*	90 °C	377 kJ/kg	1.19 $kJ/kg°C$		0.55 kg/s
8	0.7 *bara*	90 °C	1518 kJ/kg	4.34 $kJ/kg°C$	0.5	0.55 kg/s
9	0.7 *bara*	90 °C	2660 kJ/kg	7.48 $kJ/kg°C$	1	0.29 kg/s
10	2 *bara*	120 °C	2706 kJ/kg	7.13 $kJ/kg°C$	1	0.32 kg/s
11	0.7 *bara*	90 °C	377 kJ/kg	1.19 $kJ/kg°C$	0	0.06 kg/s
12	7 *bara*	90 °C	378 kJ/kg	1.19 $kJ/kg°C$		0.06 kg/s

The steam and water conditions at each numbered point in the process are presented in terms of their thermodynamic properties in Table 10. To help visualize the thermodynamic process, these values are additionally presented in a log p-h diagram in Figure 20. In this diagram, the consumption by the customer is depicted by a dashed black line, although this is not the actual thermodynamic processes of the consumption given that it is considered a black box process. The lines of the central processes in the steam generation are solid red, while dashed red lines represent separation or secondary processes.

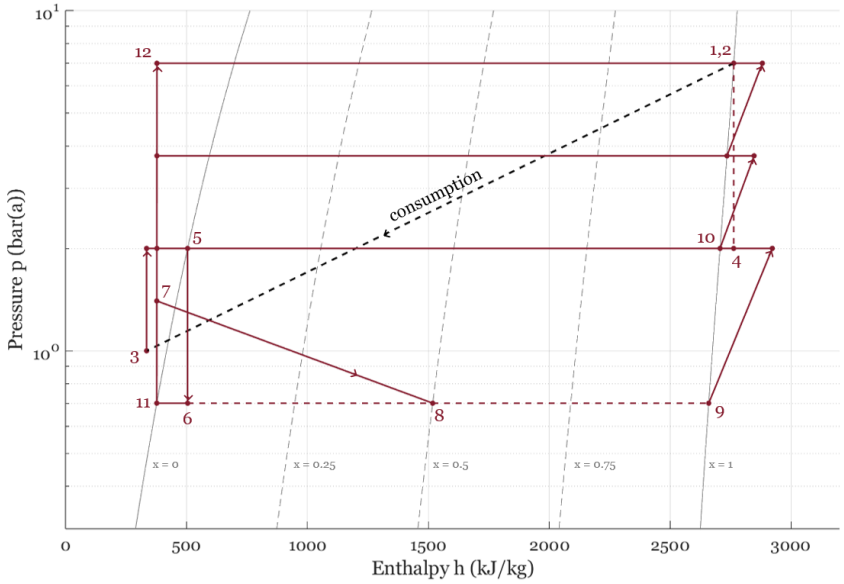

Figure 20: Log p-h diagram of the SGHP solution in Figure 19.

In the second solution with steam separation at 3.4 $bar(a)$, a larger share of the pressurization occurs prior to the evaporation as the feed water is already pumped, as illustrated in Figure 21. Compared to the previously presented solution, the main differences are in the throttle between the feed water tank and separator being replaced by a pump as well as the one screw compressor performing the whole steam pressurization without staged compression. Similarly to the first solution, the connection between the steam separator and compression heat pump includes a pump covering the 0.7 bar pressure loss of the heat exchanger. Nevertheless, since the evaporation now occurs at 3.4 $bar(a)$, or 138°C, the temperature lift of the heat pump is significantly larger which results in a lower COP and subsequently an electricity consumption more than two times larger than that of the heat pump in the first solutions. The required mass flow of the waste heat does also decrease to 9.7 kg/s or ≈ 35 t/h.

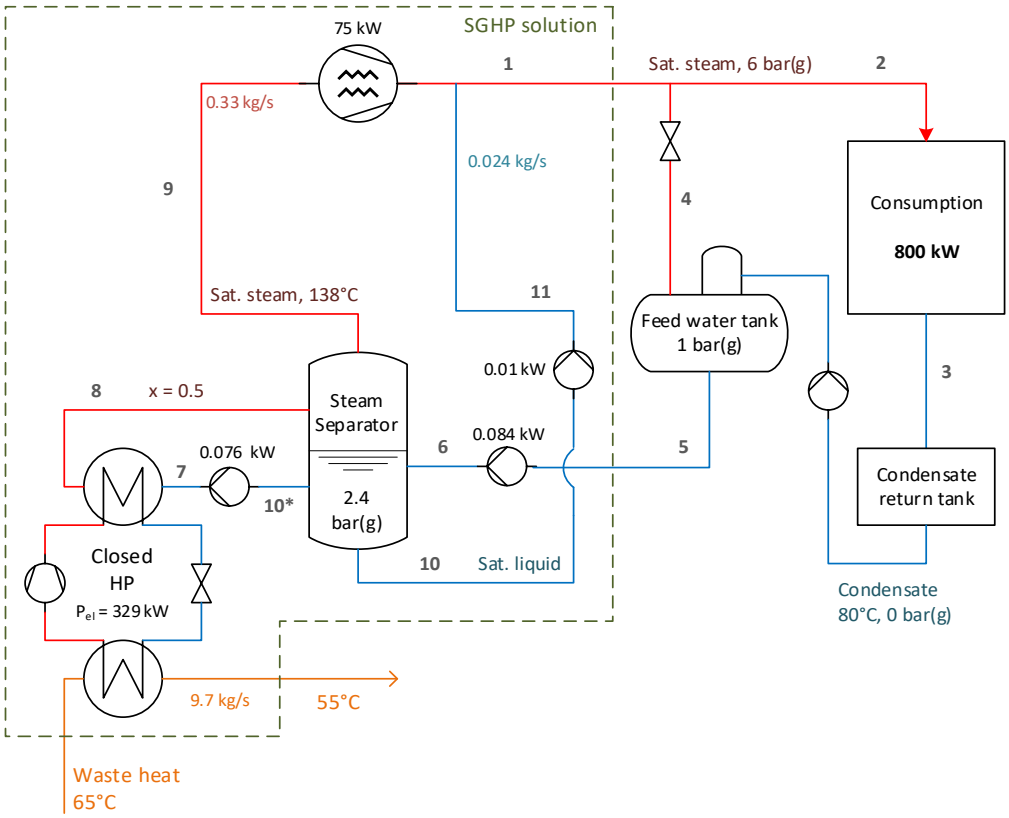

Figure 21: Flow diagram for the SGHP solution with steam separation at 3.4 bar(a) and 800kW steam production.

Table 11: Fluid conditions at each process point in Figure 21.

Process points	Pressure	Temp.	Enthalpy	Entropy	Steam fraction	Mass flow
1	7 *bara*	165 °C	2763 kJ/kg	6.71 $kJ/kg°C$	1	0.35 kg/s
2	7 *bara*	165 °C	2763 kJ/kg	6.71 $kJ/kg°C$	1	0.33 kg/s
3	1 *bara*	80 °C	335 kJ/kg	1.08 $kJ/kg°C$		0.33 kg/s
4	2 *bara*	147 °C	2763 kJ/kg	7.27 $kJ/kg°C$		0.02 kg/s
5	2 *bara*	120 °C	505 kJ/kg	1.53 $kJ/kg°C$	0	0.35 kg/s
6	3.4 *bara*	120 °C	505 kJ/kg	1.53 $kJ/kg°C$		0.35 kg/s
7	4.1 *bara*	138 °C	580 kJ/kg	1.72 $kJ/kg°C$		0.69 kg/s
8	3.4 *bara*	138 °C	1655 kJ/kg	4.33 $kJ/kg°C$	0.5	0.69 kg/s
9	3.4 *bara*	138 °C	2731 kJ/kg	6.95 $kJ/kg°C$	1	0.33 kg/s
10	3.4*bara*	138 °C	580 kJ/kg	1.72 $kJ/kg°C$	0	0.02 kg/s
11	7 *bara*	138 °C	580 kJ/kg	1.72 $kJ/kg°C$		0.02 kg/s

The calculated fluid conditions at each point in the process are specified in Table 11. The thermodynamic processes between each point are furthermore illustrated in a log p-h diagram in Figure 22. As is evident from both the flow diagram and the log p-h diagram, a higher separation pressure results in a smaller need for steam compressor and ultimately fewer compression stages and compressors. This makes the process less complex in terms of technology and maintenance, although the performance of the equipment may not be optimal.

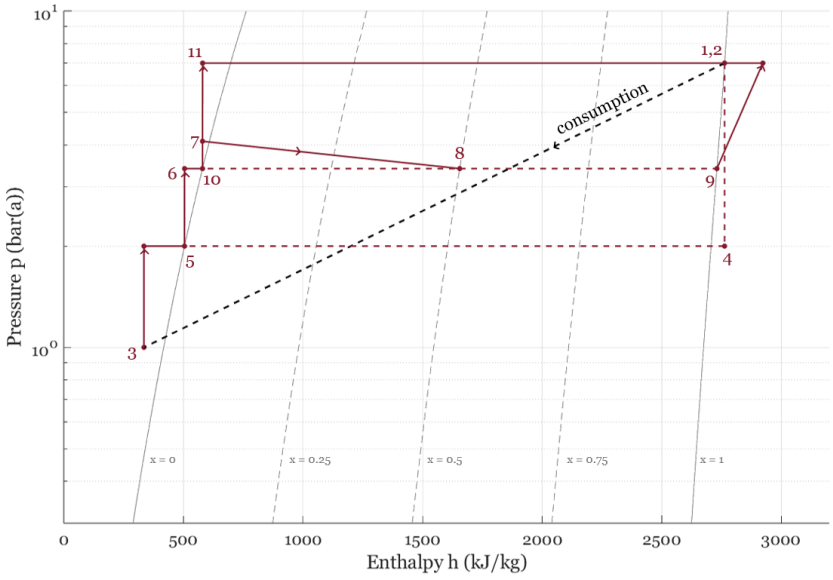

Figure 22: Log p-h diagram of SGHP solution in Figure 21.

The third example solution, illustrated in Figure 23, represents the upper boundary of possible configurations where the steam separation occurs at the supply pressure. The consumption and feed water sections of this solution are similar to the second solution described, with a pump between the feed water tank and the steam separator. The power of that pump is, however, larger as it increases the pressure all the way to 7 $bar(a)$. As a result of evaporating and separating the steam at the supply pressure, no steam compressors are required to upgrade the steam further. This makes the solution in question closer to that of boiler plants where the feedwater is normally pressurized to the desired pressure prior to evaporation in the boiler itself. The connection between the steam separator and closed cycle heat pump is, however, identical to the two previous solutions with a pump covering the pressure losses and a 50% evaporation at the heat exchanger. The high evaporation pressure also results in an even higher temperature lift demanded from the heat pump which causes the COP to drop and electrical consumption to increase further. This solution requires a waste heat mass flow of 8.8 kg/s or 31.5 t/h.

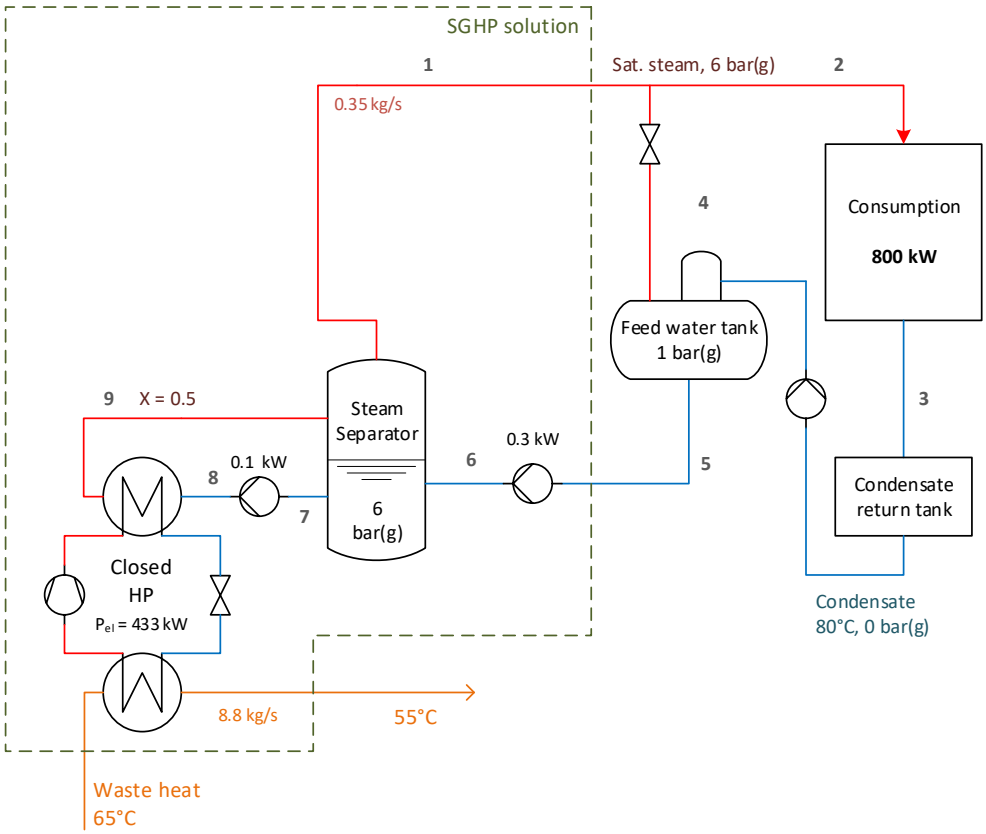

Figure 23: Flow diagram for the SGHP solution with steam separation at 7 bar(a) and 800kW steam production.

Table 12: Fluid conditions at each process point in Figure 23.

Process points	Pressure	Temp.	Enthalpy	Entropy	Steam fraction	Mass flow
1	7 $bara$	165 $°C$	2763 kJ/kg	6.71 $kJ/kg°C$	1	0.35 kg/s
2	7 $bara$	165 $°C$	2763 kJ/kg	6.71 $kJ/kg°C$	1	0.33 kg/s
3	1 $bara$	80 $°C$	335 kJ/kg	1.08 $kJ/kg°C$		0.33 kg/s
4	2 $bara$	147 $°C$	2763 kJ/kg	7.27 $kJ/kg°C$		0.02 kg/s
5	2 $bara$	120 $°C$	505 kJ/kg	1.53 $kJ/kg°C$	0	0.35 kg/s
6	7 $bara$	120 $°C$	505 kJ/kg	1.53 $kJ/kg°C$		0.35 kg/s
7	7 $bara$	165 $°C$	697 kJ/kg	1.99 $kJ/kg°C$		0.77 kg/s
8	7.7 $bara$	165 $°C$	697 kJ/kg	1.99 $kJ/kg°C$		0.77 kg/s
9	7 $bara$	165 $°C$	1730 kJ/kg	4.35 $kJ/kg°C$	0.5	0.77 kg/s

Table 12 elaborates on the state of the steam at each point in the process defined in the flow diagram. Eliminating the need for steam compression further simplifies the steam generation system and configuration which can also be seen in Figure 24. The log p-h diagrams of both the second and third solutions also illustrate that the processes in these cases never go below the 10^0 bar or 1 bar line which means that no parts of the process occur at sub-atmospheric pressures, in contrast to the first solution. This design aspect minimizes the risk of air leakage into the steam flow, ensuring the steam supply quality.

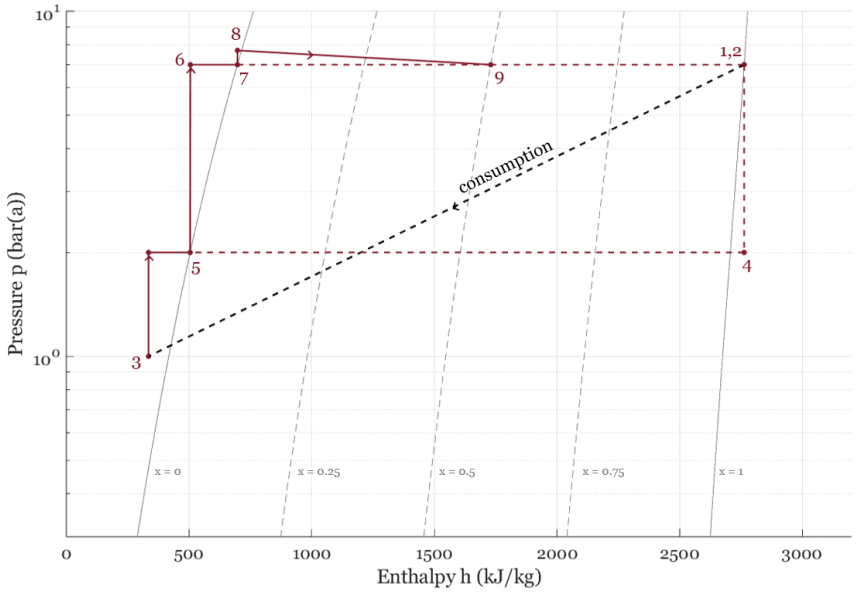

Figure 24: Log p-h diagram of SGHP solution in Figure 23.

In addition to the three solutions above, seven other configurations and balances were evaluated, in a similar manner to that described above. A summary of the different solutions evaluated is compiled in Table 13, listing the number of closed cycle compression heat pumps required as well as the thermal power demand from each, the number of steam compressors, or MVRs, required as well as the type of compressor assumed in the calculations, and the total COP or the steam generation system including all electricity consumption within the borders of the SGHP solution. These attributes of the solutions are listed in order of the steam separation pressure in each case. The COPs, calculated in accordance with the equations presented in Chapters 3.2 and 3.3, are then visualized as a function of the separation pressure in Figure 25.

Table 13: System COP calculation results for each evaluated solution.

Pressure $(bar(a))$	Nr of HP	Capacity (kW_{th})	Nr of MVR	Type(s)	**COP**
0.7	1	628	2	Screw + Piston	**2.11**
1.0	1	654	2	Screw + Piston	**2.08**
1.6	1	673	1	Screw	**2.08**
2.2	1	712	1	Piston	**1.99**
2.8	1	720	1	Screw	**2.01**
3.4	1	736	1	Screw	**1.98**
4.0	1	750	1	Screw	**1.95**
5.0	1	770	1	Screw	**1.91**
6.0	1	786	1	Screw	**1.88**
7.0	1	800	0	-	**1.85**

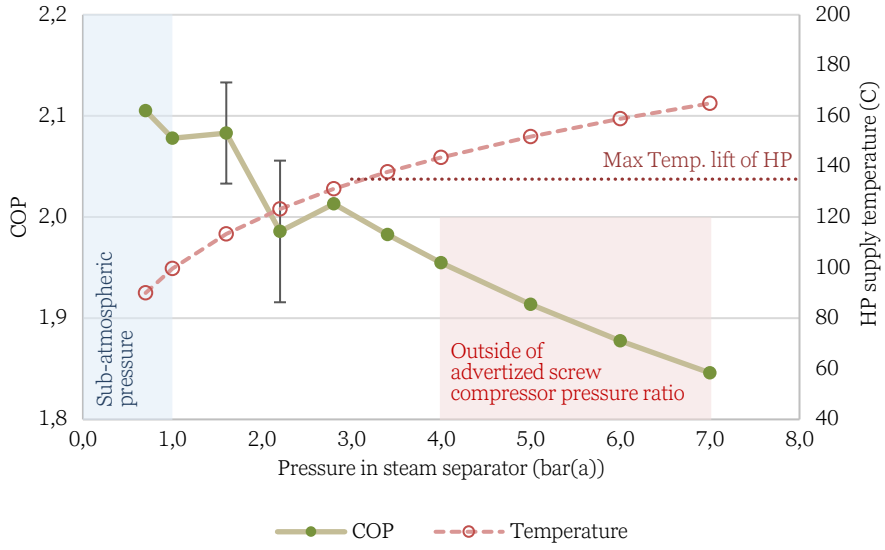

Figure 25: System COP and heat pump supply temperature visualized as a function of the steam separation pressure.

As is evident from the diagram in Figure 25, the total COP of the steam generation system decreases when the steam separation pressure increases, and a larger share of the energy comes from the heat pump rather than MVRs. Furthermore, the inconsistency visible among the lower separation pressures can be explained by the different compressor types or combinations of compressors that through the differences in efficiencies result in an irregular curve. However, it is worth noting that although the COP decreases with higher pressures, the total difference between the lower and upper limits of the solutions evaluated is only 0.26, which means a 12 % decrease.

The figure also shows the supply temperature demand each solution requires from the closed cycle compression heat pump. As the separation pressure increases and a larger weight is but on the heat pump, the temperature it needs to supply also increases. As previously stated, the lower end limit for the solutions was set based on the minimum supply temperature of the Heaten HeatBooster at $90°C$. The upper limit is however determined by the steam separation pressure of 7 $bar(a)$ which sets the supply temperature to be equal to the evaporation temperature of water at that pressure or $165°C$.

Although COPs can be calculated for all solutions between $0.7 - 7\ bar(a)$, not all of them are realistic and possible in practice due to limitations of the equipment used. The first aspect that limits some of the solutions is the pressure ratio of the compressors. The Atlas Copco screw compressor used in some of the solutions is advertised to have a possible pressure ratio of $1.8 - 6$. In the solutions with steam separation above $4\ bar(a)$, the compression requirement to upgrade the steam to the supply pressure is less than the lower end of that range. Secondly, the HeatBooster has a maximum temperature lift per stage of $80K$ at these conditions. Given that the waste heat is returning at $55°C$, the highest supply temperature one heat pump can reach is $135°C$ which additionally limits the realization of the solutions above $\approx 3\ bar(a)$ in which the required evaporation temperatures exceed this limit. Additionally, the calculated thermal capacity of the heat pump is below the advertised minimum power of the HeatBooster of 800 kW in all but one scenario. This is, however, not seen as a limitation for the possibility of realizing the designs as it can be replaced with a smaller and better fitted heat pump when the solutions are developed further in more detail.

Given these limitations, the realistic range of solutions can be narrowed down to separation pressures between $0.7 - 3\ bar(a)$. Looking at the remaining scenarios as well as their equipment requirements, two system designs can be highlighted as recommended solutions. The solutions in question are at separation pressures of $1.6\ bar(a)$ and $2.2\ bar(a)$. The recommendation is based on these systems only requiring one compressor which reduces investment costs in comparison to the solutions at lower pressures while maintaining a similar level of COP. The first solution includes a screw compressor while the latter uses a piston compressor. Although the COP of the piston

compressor solution is lower, it cannot be ruled out given the uncertainty in the isentropic and total efficiencies on the compressors. To account for the uncertainty a sensitivity analysis is conducted with the estimated efficiencies being varied by $\pm$ 5%. The results of the sensitivity analysis are displayed as error bars for the two scenarios in Figure 25.

For the two recommended solutions and their feasibility to be further evaluated, the location of installation becomes a relevant factor. Since one of the primary motivations for replacing a boiler with heat pump solution is to eliminate fossil fuel consumption and therefore reduce CO_2 emissions, the carbon intensity of the electricity used by the heat pumps affects the total abatement that can be reached. When compared to a theoretical abatement of 100% through fully renewable electricity consumption, installations in Sweden and Finland, with electrical grids with the large majorities coming from fossil free sources, can reach high abatement percentages of approximately 99% and 94%, respectively. With the EU average electricity having a significantly higher carbon intensity, an installation with this electricity would have a clearly lower effect on emission abatement with the total reduction only reaching approximately 70%.

4.2 High power steam demand

The reference process with the higher power demand requires a steam supply of $20MW$ at $4\ bar(a)$. Similarly to the low power demand, three examples are presented to show the concepts of solution with which this steam can be produced through a heat pump system. In the three examples, the steam separation occurs at $0.7\ bar(a)$, $2.8\ bar(a)$, and $4\ bar(a)$, with the minimum supply temperature of the heat pump and consumer's pressure dictating the lower and upper limits. Since the thermal power of this system is significantly larger, the mass flows of steam will also increase to almost $30\ t/h$, although the pressure is lower. As a result of the higher mass flows, the compressor selected for all solutions in this scenario is the Piller VapoMaxX centrifugal compressor. The closed cycle heat pump used in the calculations is the Heaten HeatBooster in these solutions as well. In this scenario the waste heat available to the heat pumps is warmer than in the previous solutions with the temperature at $75°C$.

As mentioned, the first solution is dictated by the $90°C$ minimum supply temperature of the Heatbooster which corresponds to an evaporation pressure of $0.7\ bar(a)$. The example solution designed around this detail can be found visualized in a flow diagram in Figure 26. With the steam separation pressure being lower than that of the feed water, a throttle is placed between the two in which the pressure is lowered to $0.7\ bar(a)$. This pressure decrease also causes a small portion of the water to evaporate resulting in the flow

entering the separation vessel to have a steam fraction of ≈ 0.06. The connection between the steam separator and heat pump is similar to the loops in the lower steam power demand scenarios with a pump to cover the pressure losses. Although illustrated as one heat pump, due to the large mass flow, this system requires seven separate heat pumps in parallel to cover the supply demand, assuming the maximum thermal power of $2.5\,MW$ of the HeatBooster. This means that the mass flow between points 7 and 8 in the process is split up to seven smaller steams all directed to separate heat pump heat exchangers. Similarly, the waste heat stream is divided and directed to separate heat pumps with the total required mass flow reaching $530\,t/h$. The generated steam exiting the steam separator is then compressed in three stages in centrifugal compressors, each increasing the pressure with a pressure ratio of ≈ 1.8. After each stage the steam is de-superheated using the condensate from the bottom of the steam separator.

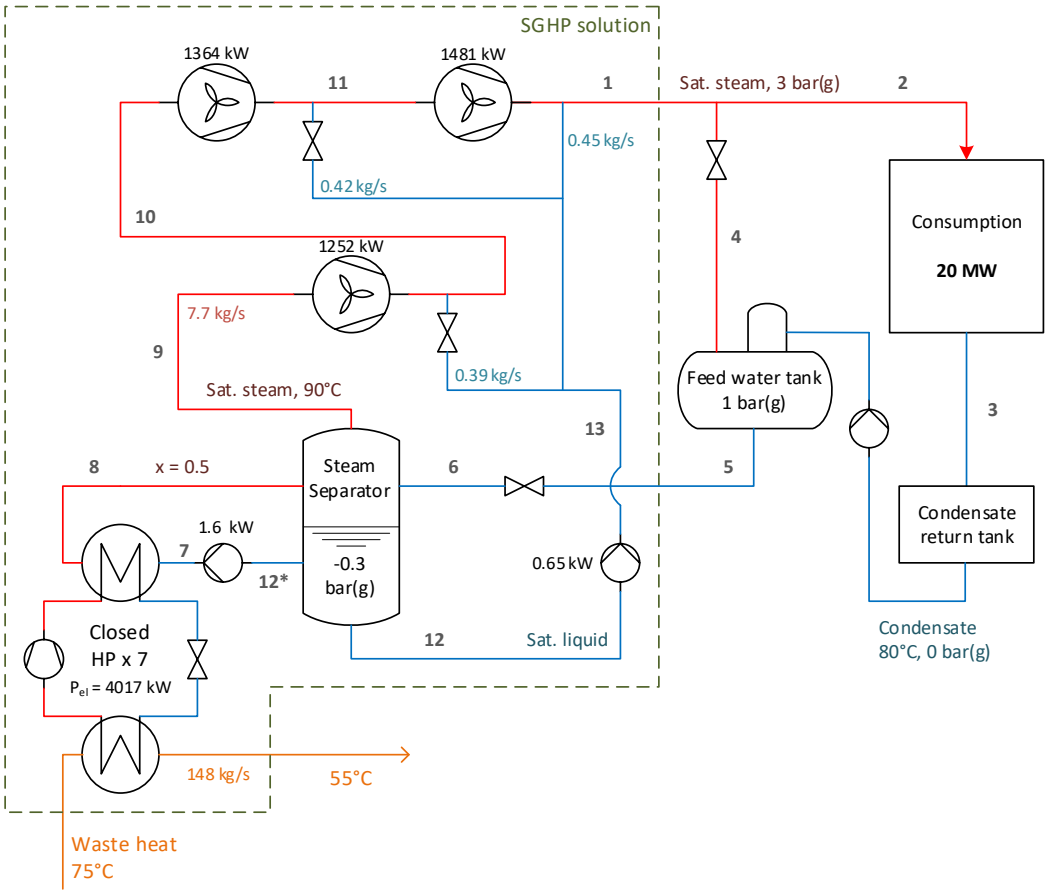

Figure 26: Flow diagram for the SGHP solution with steam separation at 0.7 bar and 20MW steam production.

Table 14: Fluid conditions at each process point in Figure 26.

Process points	Pressure	Temp.	Enthalpy	Entropy	Steam fraction	Mass flow
1	4 *bara*	144 °C	2738 kJ/kg	6.90 $kJ/kg°C$	1	8.9 kg/s
2	4 *bara*	144 °C	2738 kJ/kg	6.90 $kJ/kg°C$	1	8.3 kg/s
3	1 *bara*	80 °C	335 kJ/kg	1.08 $kJ/kg°C$		8.3 kg/s
4	2 *bara*	135 °C	2738 kJ/kg	7.21 $kJ/kg°C$		0.6 kg/s
5	2 *bara*	120 °C	505 kJ/kg	1.53 $kJ/kg°C$	0	8.9 kg/s
6	0.7 *bara*	90 °C	505 kJ/kg	1.53 $kJ/kg°C$	0.056	8.9 kg/s
7	1.4 *bara*	90 °C	377 kJ/kg	1.19 $kJ/kg°C$		14.4 kg/s
8	0.7 *bara*	90 °C	1518 kJ/kg	4.34 $kJ/kg°C$	0.5	14.4 kg/s
9	0.7 *bara*	90 °C	2660 kJ/kg	7.48 $kJ/kg°C$	1	7.7 kg/s
10	1.3 *bara*	106 °C	2685 kJ/kg	7.28 $kJ/kg°C$	1	8.1 kg/s
11	2.2 *bara*	124 °C	2712 kJ/kg	7.09 $kJ/kg°C$	1	8.5 kg/s
12	0.7 *bara*	90 °C	377 kJ/kg	1.19 $kJ/kg°C$	0	1.3 kg/s
13	4 *bara*	90 °C	377 kJ/kg	1.19 $kJ/kg°C$		1.3 kg/s

In Table 14 the fluid conditions are compiled for all numbered points in the process in terms of its thermodynamic properties. The thermodynamic processes taking place between these points are further visualized in a log p-h diagram in Figure 27. A solution with three compression stages results in a relatively complex diagram in which the black dashed line depicts the black box process of the heat consumption while the solid and dashed red lines represent the steam production itself and the supporting processes, respectively.

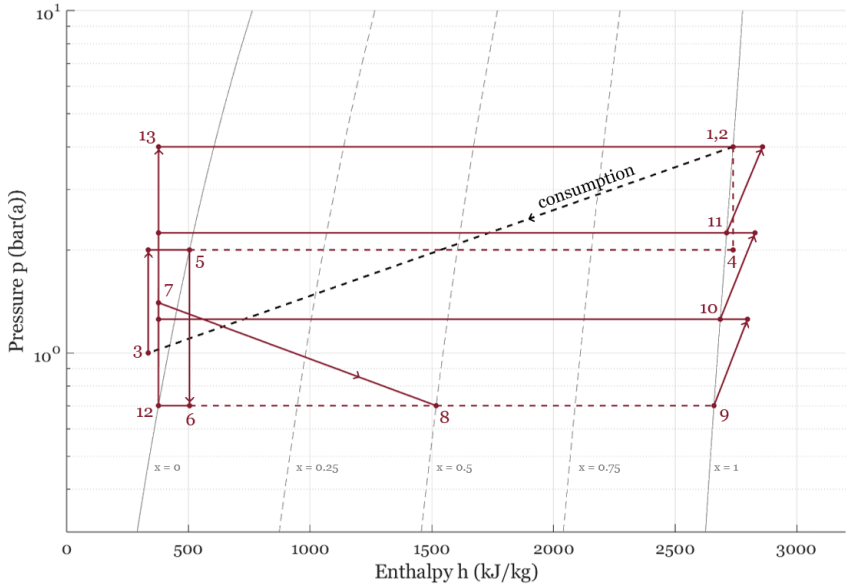

Figure 27: Log p-h diagram of SGHP solution in Figure 26.

When the steam separation pressure is increased to 2.8 $bar(a)$ and the throttle between points 5 and 6 in the process is replaced with a pump, the steam generation system can be simplified in terms of compression, with an example of a solution presented in Figure 28. In this solution the steam compression can be accomplished with one centrifugal compressor with a pressure ratio of 1.2 after which the steam is de-superheated using condensate from the steam separator. However, when lowering the compression requirements, the heat pump will need to cover the difference, resulting in a higher power demand and in this case an additional HeatBooster heat pump of 2.5 MW. The eight heat pumps connected in parallel now also consume double the electricity of that in the previous solution. The total waste heat stream required by the heat pumps decreases to approximately 480 t/h compared to the first solution.

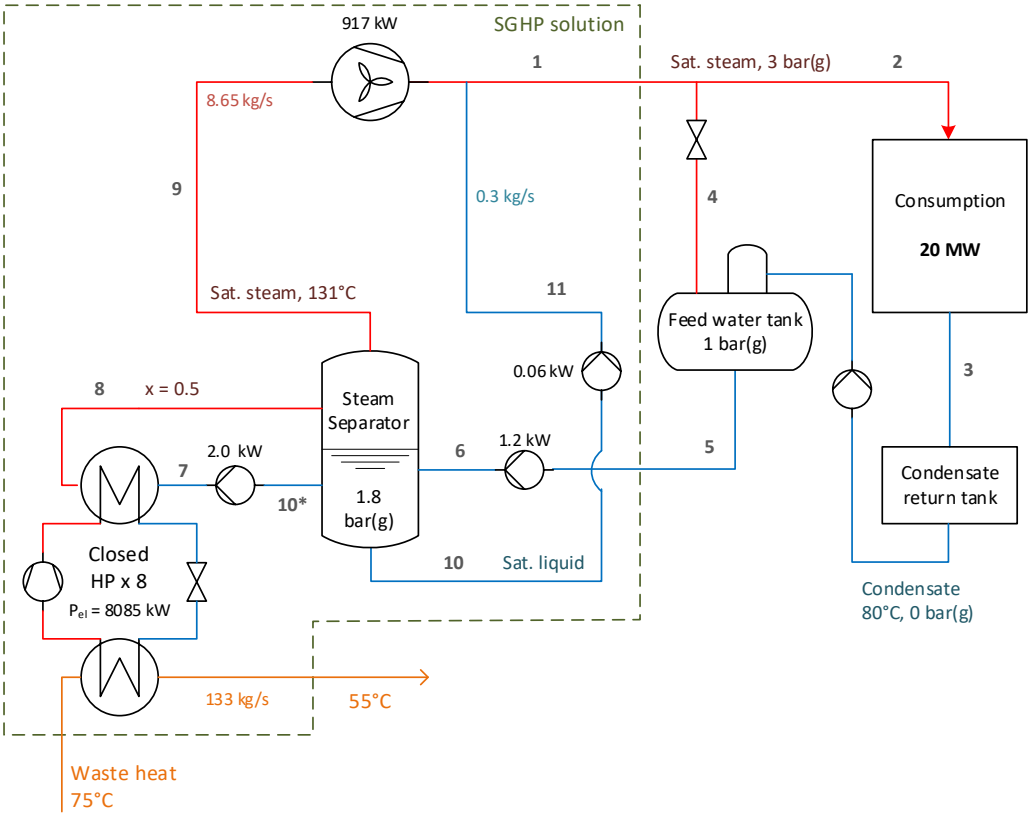

Figure 28: Flow diagram for the SGHP solution with steam separation at 2.8 bar and 20MW steam production.

Table 15: Fluid conditions at each process point in Figure 28.

Process points	Pressure	Temp.	Enthalpy	Entropy	Steam fraction	Mass flow
1	4 *bara*	144 °C	2738 kJ/kg	6.90 $kJ/kg°C$	1	8.9 kg/s
2	4 *bara*	144 °C	2738 kJ/kg	6.90 $kJ/kg°C$	1	8.3 kg/s
3	1 *bara*	80 °C	335 kJ/kg	1.08 $kJ/kg°C$		8.3 kg/s
4	2 *bara*	135 °C	2738 kJ/kg	7.21 $kJ/kg°C$		0.6 kg/s
5	2 *bara*	120 °C	505 kJ/kg	1.53 $kJ/kg°C$	0	8.9 kg/s
6	2.8 *bara*	120 °C	505 kJ/kg	1.53 $kJ/kg°C$		8.9 kg/s
7	3.5 *bara*	131 °C	552 kJ/kg	1.65 $kJ/kg°C$		17.7 kg/s
8	2.8 *bara*	131 °C	1637 kJ/kg	4.33 $kJ/kg°C$	0.5	17.7 kg/s
9	2.8 *bara*	131 °C	2722 kJ/kg	7.01 $kJ/kg°C$	1	8.6 kg/s
10	2.8 *bara*	131 °C	551 kJ/kg	1.65 $kJ/kg°C$	0	0.3 kg/s
11	4 *bara*	131 °C	552 kJ/kg	1.65 $kJ/kg°C$		0.3 kg/s

The steam and water flows at each numbered point in the process are defined and listed in Table 15 and visualized in a log p-h diagram in Figure 29. With a single compression stage this process is again visibly less complex than the first one. In addition to its simplicity, it also has the advantage of maintaining a pressure above 1 $bar(a)$, which similarly to the second and third solution example of the low power scenario, significantly reduces the risk of air leakage.

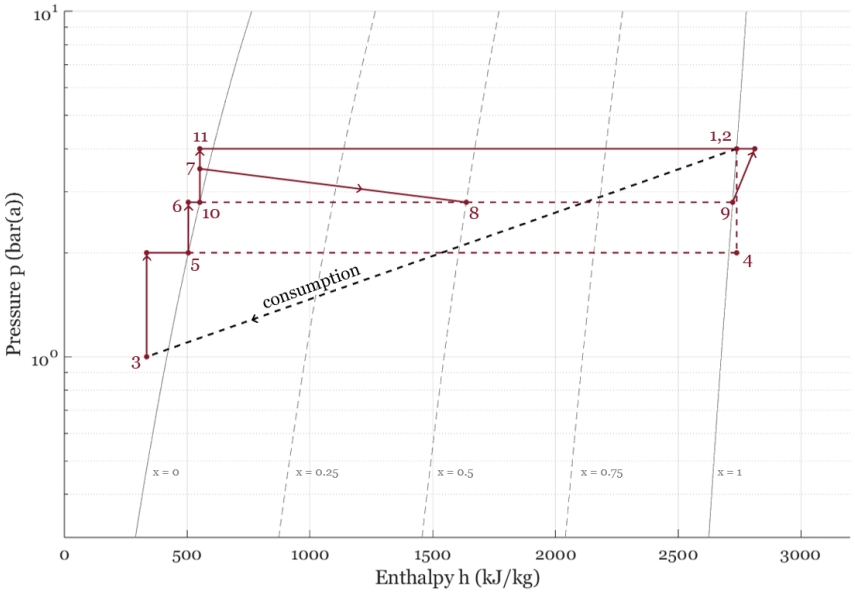

Figure 29: Log p-h diagram of SGHP solution in Figure 28.

The third solution for the high power steam demand scenario is, as mentioned, based on steam separation at the supply pressure. This concept, comparable to the concept of boilers, relies on the feed water being pressurized through pumping prior to evaporation and eliminates the need for steam compressors, as can be seen in Figure 30. In this case, the evaporation occurs, in eight separate heat pumps and their respective heat exchangers. Although the number of heat pumps in this solution is equal to the previous design, the electrical consumption is higher as all eight pumps are now calculated to operate at the maximum capacity of 2.5 MW_{th}. The requirement for the waste heat stream further decreases to less than 460 t/h. Since no additional compression is required, the saturated steam exiting the top of the steam separator is directly supplied to the consumer.

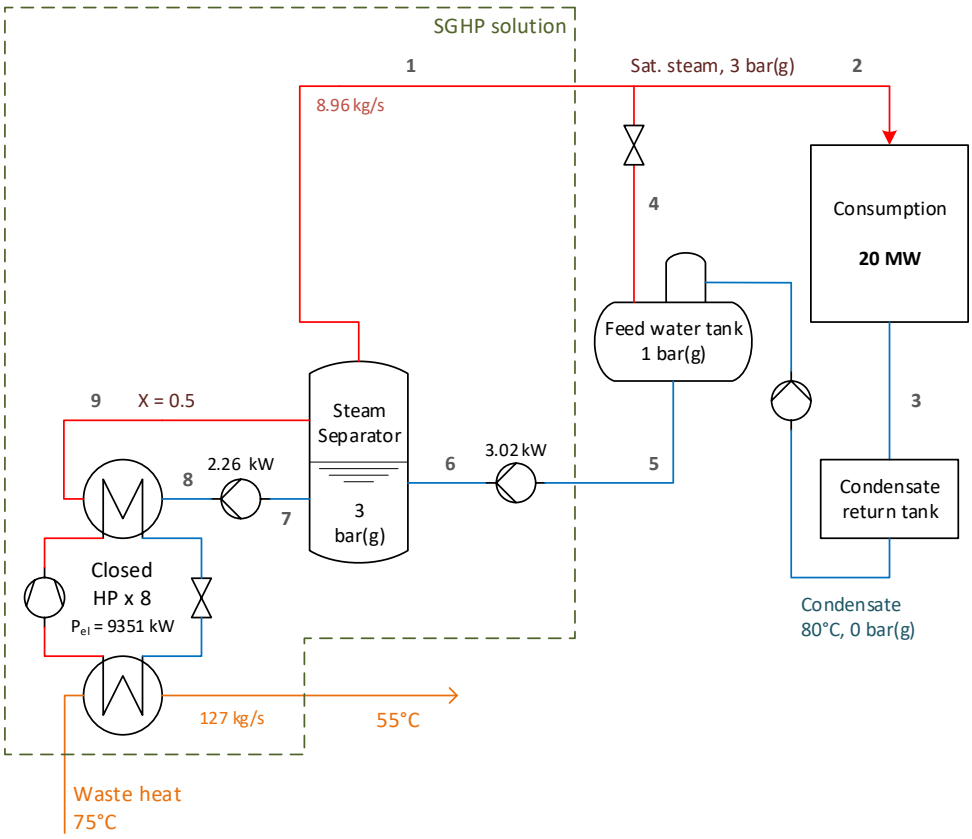

Figure 30: Flow diagram for the SGHP solution with steam separation at 4 bar and 20MW steam production.

Table 16: Fluid conditions at each process point in Figure 30.

Process points	Pressure	Temp.	Enthalpy	Entropy	Steam fraction	Mass flow
1	4 *bara*	144 °C	2738 kJ/kg	6.90 $kJ/kg°C$	1	8.9 kg/s
2	4 *bara*	144 °C	2738 kJ/kg	6.90 $kJ/kg°C$	1	8.3 kg/s
3	1 *bara*	80 °C	335 kJ/kg	1.08 $kJ/kg°C$		8.3 kg/s
4	2 *bara*	135 °C	2738 kJ/kg	7.21 $kJ/kg°C$		0.6 kg/s
5	2 *bara*	120 °C	505 kJ/kg	1.53 $kJ/kg°C$	0	8.9 kg/s
6	4 *bara*	120 °C	505 kJ/kg	1.53 $kJ/kg°C$		8.9 kg/s
7	4 *bara*	144 °C	605 kJ/kg	1.78 $kJ/kg°C$	0	18.7 kg/s
8	4.7 *bara*	144 °C	605 kJ/kg	1.78 $kJ/kg°C$		18.7 kg/s
9	4 *bara*	144 °C	1671 kJ/kg	4.33 $kJ/kg°C$	0.5	18.7 kg/s

Table 16 compiles the specifications for the steam and water flows at each numbered point in the process. The fluid conditions and thermodynamic processes are further visualized in a log p-h diagram in Figure 31, which also shows the further simplification of the steam generation system compared to earlier solutions for this scenario. This process also avoids subatmospheric pressures, therefore reducing the risk of air leakage into the process steam flows.

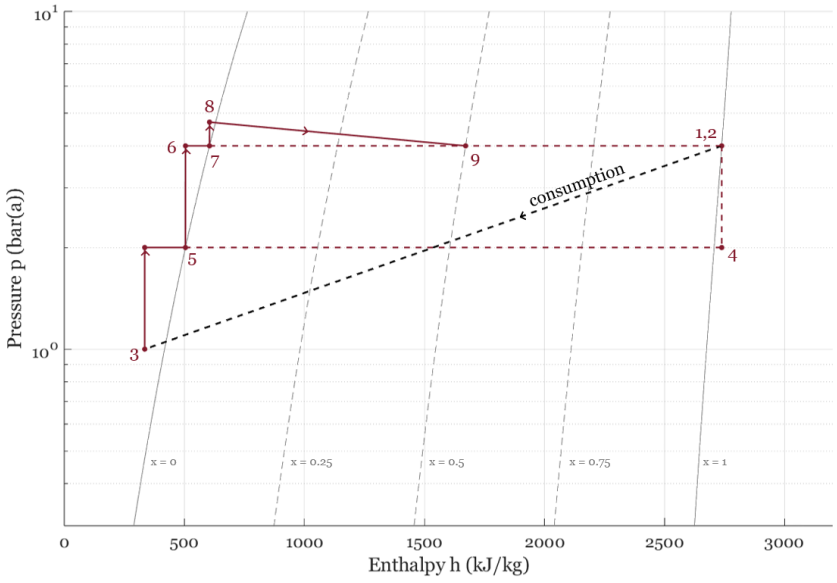

Figure 31: Log p-h diagram of SGHP solution in Figure 30.

In addition to the three solutions above, four more pressure levels in the steam separator are considered and evaluated in terms of total COP for the system within the solution boundary. The results of the calculation done in accordance with the equations presented in Chapters 3.2 and 3.3 are compiled in Table 17. For all solutions, the number of heat pumps the system requires is based on the maximum thermal power of the HeatBooster and, therefore, the number presented in the table should be rounded up to an integer to obtain the real quantity. The COPs for each solution are visualized, along with the required supply temperature from the heat pump, as a function of the steam separation pressure in Figure 32.

Table 17: System COP calculation results for each evaluated solution.

Pressure $(bar(a))$	Nr of HP	Capacity (kW_{th})	Nr of MVR	Type(s)	**COP**
0.7	6.6	2500	3	Centrifugal	**2.46**
1.0	6.8	2500	3	Centrifugal	**2.42**
1.6	7.2	2500	2	Centrifugal	**2.34**
2.2	7.5	2500	2	Centrifugal	**2.27**
2.8	7.7	2500	1	Centrifugal	**2.22**
3.4	7.9	2500	1	Centrifugal	**2.18**
4.0	8.0	2500	0	-	**2.14**

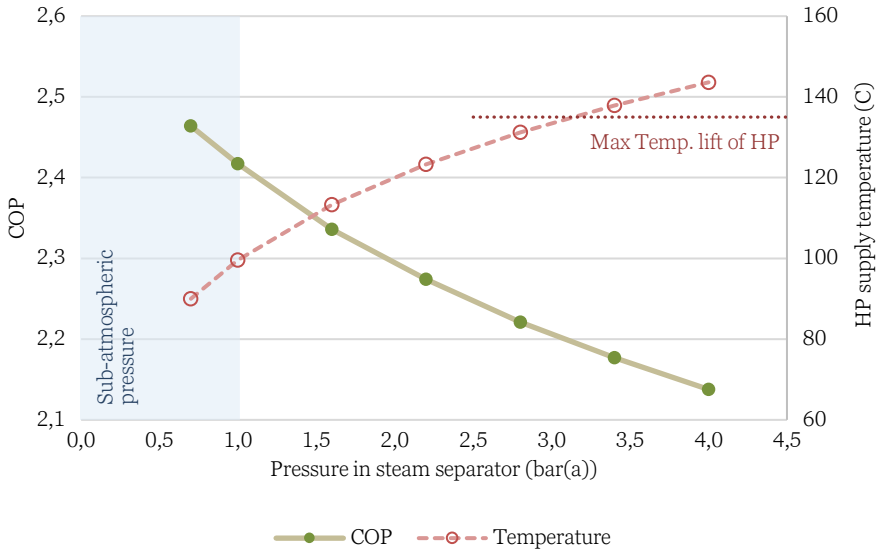

Figure 32: System COP and heat pump supply temperature visualized as a function of the steam separation pressure.

Similarly to the low power steam demand scenario, the COP of these solutions decrease as the steam separation pressure becomes larger with the highest COP at 0.7 bar of almost 2.5, as can be seen in Figure 32. However, since all solutions here are based on the same compressor equipment the curve adopts a more continuous form. Between the lowest and highest separation pressures, the total COP decreases by 0.32 or approximately 13%, although the difference in pressure between the lower and upper extremes is smaller than in the previous scenario. The supply temperature of the heat pump in this scenario behaves the same as in the previous. Nevertheless, the lower steam supply pressure also results in the upper limit temperature being lower at only approximately $144°C$.

Additionally, the lower supply pressure and temperatures mean that equipment limitations become less relevant. The return temperature of the available waste heat stream at $55°C$ together with the $80\ K$ maximum temperature lift of the heat pump sets the supply limit to $135°C$, which only eliminates the few highest-pressure solutions. Furthermore, the centrifugal compressors are not advertised to have a lower limit for the pressure ratio. Even though the equipment may allow for solutions with larger steam separation pressures, the recommended solution for this scenario is based on a steam separation at atmospheric pressure. The recommendation can be motivated by this solution only requiring seven heat pumps and avoiding the risk of air leakage. Nevertheless, it requires three compressors, operating with a pressure ratio of ≈ 1.6, as opposed to the following solution, however, it provides a higher COP, and the compressor is furthermore assumed to have a lower investment cost compared to an additional closed cycle heat pump.

Although this solution is the recommended one out of the evaluated alternatives from a technological efficiency perspective, its feasibility in terms of CO_2 abatement efficiency is also dependent on the location of installation. In Finland and Sweden with low carbon intensity electricity, replacing a natural gas boiler of the reference size with the recommended heat pump solution would reduce the total emissions with 94% and 99%, respectively, when compared to a 100% abatement in the case of fully renewable and green electricity. Electricity used would correspond to the average electricity within the European union in terms of carbon intensity, the net abatement would only amount to 69%.

4.3 Financial perspective

In order for a solution to be realistic and a real alternative for industries, the technical feasibility itself is not sufficient. Instead, financial profitability drives the decisions on what solutions and systems are integrated into the industrial processes. Therefore, in order for the SGHP solutions to be realistic alternatives for fossil fuel boilers, the annual savings they generate need to be sufficiently large to cover the required investment costs over a specified amount of time and generate actual savings and profits after that. In this thesis the desired payback time is set to be 6 years. As per the equations presented in chapter 3.4, the savings and thus the financial profitability rely on both fuel and electricity prices. The results of the financial evaluation of the solutions are presented in Figure 33, with annual savings for the recommended solutions at 1.6 $bar(a)$ and 1 $bar(a)$ for the 800 kW and 20MW scenarios, respectively, as well as the maximum investment the savings lead to. The error bars at the max CAPEX illustrate the range of investments calculated for all solutions with sub-atmospheric separation pressures allowing for the largest investments. The following paragraphs further elaborate on how the national and local differences in fuel and energy prices impact the financial profitability of the SGHP solutions evaluated.

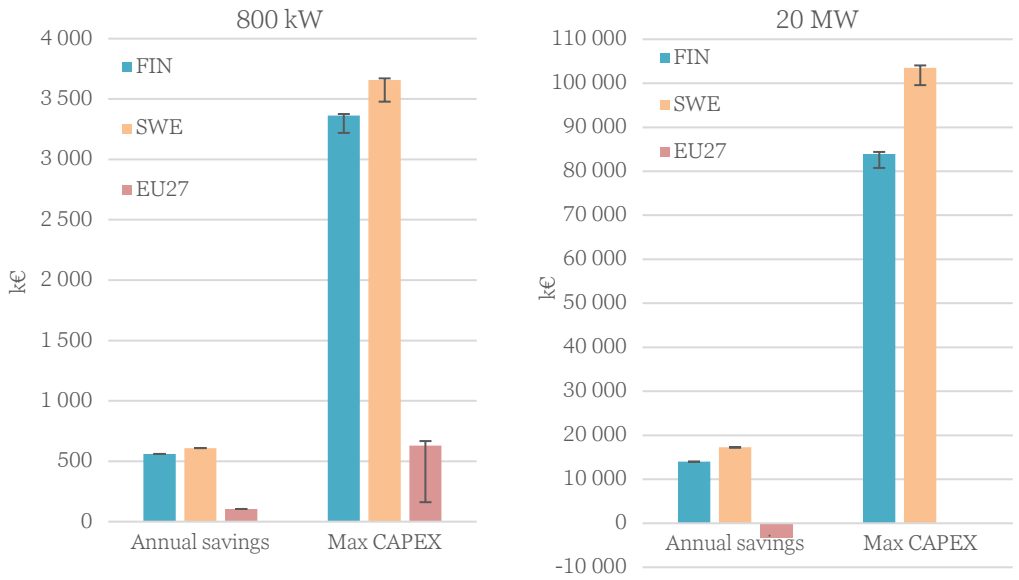

a) b)

Figure 33: Annual savings and maximum investment costs for a 6-year payback time for solutions in a) the low-capacity scenario at 800 kW and b) the high-capacity scenario at 20 MW.

In Finland, the relatively low electricity prices and higher fossil fuel prices lead to noticeable savings in both capacity scenarios. In the 800 kW scenario the annual savings amount to approximately 560 $k€$ which results in a CAPEX limit of ≈ 3.4 $M€$. When compared to the prices of heat pumps and other equipment, this investment limit may drive the choice of solution to one with a higher separation pressure and therefore less demand for compressors. The range of the CAPEX calculations for all ten solutions in this case is 160 $k€$. For the larger solutions of 20 MW annual savings reach approximately 14 $M€$. These savings allow for an investment close to 84 $M€$ for the recommended solution and a range of 3.6 $M€$. With investments possible up to 84$M€$, CAPEX savings from reducing the number of compressors become less relevant.

Both fuel and electricity prices are slightly higher in Sweden compared to Finland, however, with the fuel prices specifically being more than 10€ higher per MWh, the savings in both scenarios also grow larger than in Finland. For the low power recommended solution, the annual savings reach approximately 610 $k€$ which amounts to a maximum of almost 3.7 $M€$ in CAPEX. The range of CAPEX for other solutions is 190$k€$. Although, they are somewhat larger than for the Finnish installations, they still set similar limitations on the equipment selections and the choice of solutions. For the 20MW solutions, the recommended solution generates annual savings at approximately 17 $M€$ and a subsequent investment limit of 103 $M€$. In Sweden the range of CAPEX for the different solutions, however, reach 4.5 $M€$ which is a result of the higher electricity price and the larger relevance of COP this leads to.

When the financial evaluations for installations in the Nordic countries are compared to European averages, the differences are evident. With electricity prices generally higher in the rest of Europe, the savings a steam generating heat pump solution can generate drop. When the financials of the low-capacity scenario recommended solution are calculated with EU average prices, the annual savings are only slightly over 100 $k€$. The lower savings also result in a possible CAPEX of only 630 $k€$ while the expensive electricity increases the range to 506 $k€$ compared to Finland and Sweden. Furthermore, natural gas is significantly more affordable in the EU on average than in the Nordics. This, when combined with the higher electricity prices, leads to significantly lower savings and worse financial profitability. In the case of the 20 MW recommended solution, the calculated savings are negative, meaning that the solution does not generate any savings but rather has higher operating costs compared to the gas boiler. Therefore, no CAPEX limit is calculated for this scenario and location.

The results of the financial evaluation highlight the location dependency of the overall feasibility of a heat pump solution. It is evident that low electricity prices are essential for heat pumps to be profitable while fuel

prices also need to be higher, either alone or through CO_2 prices driving up the total cost of using fossil fuel boilers. The specific CAPEX limits for the recommended solutions in Sweden are $4.60\ €/kW$ and $5.20\ €/kW$ for the smaller and larger processes, respectively. In Finland, however, both scenarios have a specific CAPEX limit of $4.20\ €/kW$, which suggests that the difference is not a result of economy of scale but rather the fuel prices of LFO and natural gas relative to each other. Economy of scale is more likely to have an impact on required CAPEX, rather than operational savings.

4.4 Discussion

Comparing the results obtained from both steam demand scenarios and their respective solutions provides insight into what aspects affect the feasibilities as well as the relevance of them. The largest difference between the two in terms of technical feasibility is the difference in COPs the solutions are able to reach. The low power steam demand solution with the higher COP reaches 2.11 at a separation pressure of 0.7 bar while even the least efficient solution of the higher power steam demand scenario at 4 bar reaches a higher COP of 2.14, although only marginally. The inconsistency can be explained by the difference in supply pressures of 7 $bar(a)$ and 4 $bar(a)$. This results in the smaller reference process having higher pressure, and thus higher temperature targets for the steam supply which need to be covered by the steam generation system, thus lowering the COP.

Although the COPs vary between the two scenarios, emission abatements are close to identical. They cannot, however, be directly compared to each other since the recommended solutions are not based on the same pressure difference, and the difference in COP also directly implies differences in electricity consumption. Furthermore, the reference processes operate on different fuels. When the abatement percentage is calculated for the larger power scenario using a COP of 2, in order to remove the effect of efficiency form the calculations and comparison, the reductions drop slightly, however, only by a few units at most. This small drop can be explained by natural gas used in the larger scenario being less carbon intensive compared to light fuel oil. However, the main implication of this is that the carbon intensity of the electricity in the heat pump solution has a higher relevance from the net abatement perspective over efficiencies or fuel types.

Furthermore, the results in both scenarios illustrate that a higher COP can be reached when steam separation occurs at a lower pressure setting lower demands on the heat pump and upgrading the produced steam in steam compressors instead. The best and most recommended solutions in both scenarios require closed cycle heat pump supply temperatures below $120°C$. According to a review lead by the Danish Technology Institute,

VHTHP with capacities up to 10 MW and supply temperatures up to 120°C are estimated to reach commercial roll-out and be established as preferred technology by 2025 and 2026 (Poulsen and Arpagaus, 2024). This indicates that the technologies required for the recommended solutions are in line with available technology today. Therefore, technical development is unlikely to limit technological feasibility. It is, however, worth noting that the reliability of the literature reviewed may be somewhat limited due to unverified product and supplier data having been used.

In the solutions evaluated in this thesis it is assumed that sufficient waste heat flows are available. If this is not the case, steam generating heat pumps can also be installed alongside an electric boiler, for example. Through parallel steam consumption from a heat pump and a boiler, loads can, furthermore, be optimized to cover base load from the heat pump system while a more flexible boiler is able to answer to peak load and variations in the real consumption. This also allows for further optimization of efficiency and profitability.

When compared to a steam generation system based solely on electric boilers, which in terms of cutting out the consumption of fossil fuels serves the same purpose as SGHP solutions, a heat pump based steam generation system will additionally cut electricity consumption by more than half, in the case of a COP of 2. With global and especially European fuel and electricity markets experiencing increasing instability due to international conflicts, such as the sudden cut and reduction in natural gas imports into the EU which resulted in the 2022 energy crisis, a lower electricity consumption also diminishes the effects of price fluctuations. In areas with limited availability in the electric grid, the low electricity demand per unit of steam generated may also improve opportunities and feasibilities.

While SGHP solutions can create a buffer towards high electricity prices, the profitability of these installations is highly dependent on a reliable supply of affordable electricity. The results suggest that Swedish energy prices are favorable for heat pump based solutions. However, given that the electricity price used in the evaluation is a national average, although the balance between supply and demand is generally significantly different in the different Swedish price zones, an installation in SE1 or SE2 where electricity prices are typically lower, may result in better profitability and larger savings.

Similarly, the profitability can improve if operating costs of the existing boiler rise. This can either happen due to a fuel shortage such as that of the 2022 energy crisis. Alternatively, it can grow through increased costs of emission allowances, assuming the site and production is covered by the EU ETS, or as a result of stricter national carbon taxation. Especially changes in emissions and carbon prices are generally relatively slow which makes this aspect unlikely to cause a significant improvement to the business case of steam generating heat pumps. Instead, investments and further development can be made more attractive in the industrial sector through subsidy schemes

shortening the payback times of these solutions and support the decarbonization of industrial heat production.

Although heat pumps do not have extensive history in steam producing applications, considerable amounts of data, references, and research are already available to build an understanding of today's situation and future scenarios for the development. Nevertheless, the results of this study are only to be used as an indication for the general feasibility of steam generating heat pumps in industrial applications. Since no two industrial systems are the same, a SGHP solution in terms of balance between heat pumps and boilers as well as equipment optimization should be separately reviewed and designed for every application. Some systems may also not have equally high standards for steam quality in which case air leakage may be accepted and a sub-atmospheric solution can be considered, without additional costs for sealing of the equipment and piping, to improve the COP. Furthermore, steam consumption should generally not be considered a black box when designing the integration of heat pumps into a steam generation system and replacing fossil-based steam production since additional energy and cost savings may also be possible from further process optimization and heat recovery.

5 Conclusions

With the decarbonization of industries and industrial processes behind schedule for global warming target scenarios, industrial heat pumps and steam generation systems based on these can play a significant role in phasing out the fossil energy sources used today. As suggested by the results in this thesis, heat pump based steam generation is not dependent on closed cycle heat pumps able to achieve supply temperatures well over $120°C$, which are still in development or pilot stages. Instead, steam can be successfully produced and upgraded to a desired pressure and temperature using heat pump technology that is available today, which is also verified by several references of SGHP systems available in literature. The solutions and configurations evaluated in this study are especially a viable and well performing solution when the available or preferred heat pump or heat exchanger technology does not allow for total evaporation.

Nevertheless, the results of this study also highlight the drawback slowing down the industrial energy transition. With insufficient fossil fuel prices, possible savings available by replacing boilers with heat pump based solutions do not reach adequate levels to motivate the use of clean energy sources and build a profitable business case for steam generating heat pumps. Supporting subsidy schemes can however promote business cases to help drive this energy transition and improve decarbonization in the industry.

Today steam generation systems with heat pumps and compressors are mainly a realistic alternative for low pressure steam production in the Nordic region with clean and affordable electricity already in the upcoming years. Moreover, the relatively small COP and subsequent added saving that a more complex configuration and solution generate indicates that a simpler solution is often to be preferred. It is also generally beneficial from a financial perspective to design steam generating heat pumps to operate above atmospheric pressure, thus guaranteeing steam quality. To conclude, the findings of this thesis can be used to guide the introduction of SGHP solutions into the industrial sectors in a technically and financially profitable way.

References

ALAKANGAS, E., HURSKAINEN, M., LAATIKAINEN-LUNTAMA, J. & KORHONEN, J. 2016. Suomessa käytettävien polttoaineiden ominaisuuksia, VTT Technology 258.

ARPAGAUS, C., BLESS, F., UHLMANN, M., SCHIFFMANN, J. & BERTSCH, S. S. 2018. High temperature heat pumps: Market overview, state of the art, research status, refrigerants, and application potentials. *Energy,* 152**,** 985–1010.

ATLAS COPCO. n.d.–a. *Atlas Copco energy conversion solutions, Industrial heat pumps and steam compressors* [Online]. Available: https://www.atlascopco.com/content/dam/atlas-copco/compressor-technique/oil-free-air/documents/energy-conversion/Energy%20conversion%20industrial%20heat%20pumps%20and%20steam.pdf [Accessed 07.01 2026].

ATLAS COPCO. n.d.–b. *Boiler Efficiency* [Online]. Available: https://www.atlascopco.com/en-us/rental/resources/industrial-steam-guide-temperature-control/industrial-steam-boilers/boiler-efficiency [Accessed 09.01 2026].

ATLAS COPCO. n.d.–c. *Industrial rotary screw oil-free steam compressors* [Online]. Available: https://www.atlascopco.com/en-my/compressors/products/energy-conversion/steam-compressor-ec [Accessed 07.01 2026].

D'ALESSANDRO, G., IEZZI, M. & DE MONTE, F. 2025. Steam Generating High Temperature Heat Pumps: Best Practices, Optimization Strategies and Refrigerant Selection for Performance Improvement. *Energies* [Online], 18.

EEA. 2025. *Greenhouse gas emission intensity of electricity generation in Europe* [Online]. Available: https://www.eea.europa.eu/en/analysis/indicators/greenhouse-gas-emission-intensity-of-1 [Accessed 25.3 2026].

ENERGIMYNDIGHETEN 2025. Oil price for industrial customers, öre/kWh, 1995-2024 (2023 prices).

ENERIN AS. n.d.–a. *HoegTemp* [Online]. Available: https://www.enerin.no/hoegtemp [Accessed 10.12 2025].

ENERIN AS. n.d.–b. *References* [Online]. Available: https://www.enerin.no/references [Accessed 10.12 2025].

EUROPEAN COMMISSION. 2026. *Weekly Oil Bulletin* [Online]. Available: https://energy.ec.europa.eu/data-and-analysis/weekly-oil-bulletin_en [Accessed 08.04 2026].

EUROSTAT 2026a. Electricity prices for non-household consumers - bi-annual data (from 2007 onwards).

EUROSTAT 2026b. Gas prices components for non-household consumers - annual data.

GOODARZVAND-CHEGINI, F., SAMIEE, L. & RAHMANIAN, N. 2023. Energy savings from flash steam recovery: An industrial case study. *Energy Conversion and Management: X,* 19**,** 100393.
HAN, D., CHEN, J., ZHOU, T. & SI, Z. 2021. Experimental investigation of a batched mechanical vapor recompression evaporation system. *Applied Thermal Engineering,* 192**,** 116940.
HE, Z., SHEN, J., CHEN, W. & XING, Z. 2012. Design and performance evaluation of a twin screw water vapor compressor.
HEATEN 2026. HBL4-W/S Technical Data Sheet.
HEATEN. n.d.–a. *HeatBooster* [Online]. Available: https://heaten.com/products [Accessed 10.12 2025].
HEATEN. n.d.–b. *Heaten* [Online]. Available: https://heaten.com/ [Accessed 12.2 2026].
HOFMANN, M. & TSATSARONIS, G. 2015. Exergy-Based Study Of A Binary Rankine Cycle. *ECOS 2015 - The 28th International Conference on Efficiency, Cost, Optimization Simulation and Environmental Impact of Energy Systems.*
HOLMGREN, M. 2007. X Steam, Thermodynamic properties of water and steam. MATLAB Central File Exchange: The Mathworks, Inc.
HPT TCP. 2022a. *HoegTemp UHT heat pump, Enerin AS* [Online]. Available: https://heatpumpingtechnologies.org/content/uploads/sites/70/2022/07/enerin-hoegtemp.pdf [Accessed 10.12 2025].
HPT TCP. 2022b. *Micro Steam Recovery Compressor / MSRC160L, KOBELCO Compressors Corporation* [Online]. Available: https://heatpumpingtechnologies.org/content/uploads/sites/70/2022/07/technologykobelcomsrc160l-1.pdf [Accessed 07.01 2026].
HPT TCP. 2022c. *Spilling Steam Compressor, Spilling Technologies GmbH* [Online]. Available: https://heatpumpingtechnologies.org/content/uploads/sites/70/2022/07/hthpannex58suppliertechnology-spilling.pdf [Accessed 29.12 2025].
HPT TCP. 2023. *HeatBooster Heaten* [Online]. Available: https://heatpumpingtechnologies.org/content/uploads/sites/70/2023/12/hthpannex58templatesuppliertechnologyrev4-v3.pdf [Accessed 10.12 2025].
IEA. 2023a. *Industry* [Online]. Available: https://www.iea.org/energy-system/industry [Accessed 03.12 2025].
IEA 2023b. Tracking Clean Energy Progress 2023.
JOUNI, W., BEUCHER, Y. & ASSAAD, Z. Theoretical and Experimental Study of Flash Tank in a Heat Pump Based Steam Generation – Part 2. 37th International Conference on Efficiency, Cost, Optimization, Simulation and Environmental Impact of Energy Systems, 2024–07–01 2024 Rhodes (Grèce), Greece.
KLUTE, S., BUDT, M., VAN BEEK, M. & DOETSCH, C. 2024. Steam generating heat pumps – Overview, classification, economics, and basic

modeling principles. *Energy Conversion and Management,* 299**,** 117882.
LIU, G., ZHAO, X., LIANSHENG, L., BIN, T., QICHAO, Y. & YUANYANG, Z. 2019. Analysis on Performance of Screw Compressor in MVR system. *IOP Conference Series: Materials Science and Engineering,* 604**,** 012002.
MA, X., DU, Y., ZHAO, T., ZHU, T., LEI, B. & WU, Y. 2024. A comprehensive review of compression high-temperature heat pump steam system: Status and trend. *International Journal of Refrigeration,* 164**,** 218–242.
MANNING, C. G. 2023. *Technology Readiness Levels* [Online]. Nasa.gov. Available: https://www.nasa.gov/directorates/somd/space-communications-navigation-program/technology-readiness-levels/ [Accessed 10.12 2025].
MINALE, T. A., LANZETTA, F., BÉGOT, S. & GETIE, M. Z. 2024. Review on the technological advancement of Stirling cycle heat pumps. *Energy Reports,* 12**,** 3504–3518.
PILLER. 2024a. *Piller VapoFan* [Online]. Available: https://www.piller.de/fileadmin/media/pdf-files/Produkt_und_Serviceinformationen-en/vapofan-high-speed-blowers-en.pdf [Accessed 08.01 2026].
PILLER. 2024b. *Piller VapoFlex* [Online]. Available: https://www.piller.de/fileadmin/media/pdf-files/product-sheets/PILLER_VapoFlex_en.pdf [Accessed 08.01 2026].
PILLER. 2024c. *VapoMaxX* [Online]. Available: https://www.piller.de/fileadmin/media/pdf-files/Produkt_und_Serviceinformationen-en/vapomaxx-vapor-compressor-en.pdf [Accessed 08.01 2026].
PILLER. n.d. *Products and Services* [Online]. Available: https://www.piller.de/products-services/ [Accessed 08.01 2026].
POULSEN, J. L. & ARPAGAUS, C. 2024. *Task 1 - HTHP Technologies, State of the Art Review & Realized Demonstrations* [Online]. Available: https://heatpumpingtechnologies.org/content/uploads/sites/70/2024/04/finalwebinarannex58-1.pdf [Accessed 16.4 2026].
SON, Y.-J., SUH, J.-W., YANG, H., LEE, K.-Y., LEE, S.-W., YOON, J. & CHOI, Y.-S. 2021. Similarity model for predicting the performance of an R718 compressor. *Advances in Mechanical Engineering,* 13**,** 16878140211050797.
SPILLING. 2024a. *Steam Compression* [Online]. Available: https://www.spilling.de/applications-steam/steam-compression.html [Accessed 29.12 2025].
SPILLING. 2024b. *Steam Compressors* [Online]. Available: https://www.spilling.de/products/steam-compressors.html [Accessed 29.12 2025].

SPIRAX SARCO. n.d. *Learn about steam, Steam Accumulators* [Online]. Available: https://www.spiraxsarco.com/learn-about-steam/the-boiler-house/steam-accumulators [Accessed 15.1 2026].
STATISTIKMYNDIGHETEN 2026a. Priser på el för övriga kunder (ej hushåll) efter förbrukarkategori. Halvår 2014H2 - 2025H2.
STATISTIKMYNDIGHETEN 2026b. Priser på naturgas för övriga kunder (ej hushåll). Halvår 2014H2 - 2025H2.
SUONG, C. O. & ASANAKHAM, A. 2020. Evaluation of a single stage heat pump performance by figure of merit (FOM). *Energy Reports,* 6**,** 2735–2742.
TILASTOKESKUS 2026a. 12hf -- Maakaasun hinta jakeluverkkoasiakkaille (ei sis. veroja), 2021M01-2025M12.
TILASTOKESKUS. 2026b. *Energian hinnat* [Online]. Available: https://stat.fi/fi/tilasto/ehi [Accessed 2.4 2026].
VAHTERUS OY. n.d. *Evaporators* [Online]. Available: https://vahterus.com/applications/evaporators/ [Accessed 14.1 2026].
VEROHALLINTO. 2026. *Tax rates on electricity and certain fuels* [Online]. Available: Tax rates on electricity and certain fuels - vero.fi [Accessed 2.4 2026].
WANG, C., XU, R., CHEN, X., JIANG, P. & LIU, B. 2019. Study on water flash evaporation under reduced pressure. *International Journal of Heat and Mass Transfer,* 131**,** 31–40.
WEI, M., MCMILLAN, C. A. & DE LA RUE DU CAN, S. 2019. Electrification of Industry: Potential, Challenges and Outlook. *Current Sustainable/Renewable Energy Reports,* 6**,** 140–148.
WSE TURBO. n.d. *Technology* [Online]. Available: https://www.wse-turbo.com/technology/ [Accessed 08.01 2026].
YANG, J., ZHANG, C., ZHANG, Z., YANG, L. & LIN, W. 2016. Study on mechanical vapor recompression system with wet compression single screw compressor. *Applied Thermal Engineering,* 103**,** 205–211.
ZEYGHAMI, M. 2010. Thermoeconomic Optimization of Geothermal Flash Steam Power Plants. *Proceedings World Geothermal Congress 2010.*